Fraunhofer
ITWM

A. Klar, N. Marheineke, R. Wegener

Hierarchy of mathematical models for production processes of technical textiles

Berichte des Fraunhofer ITWM, Nr. 156 (2009)

ISSN 1434-9973

Bericht 156 (2009)

Die Veröffentlichungen in der Berichtsreihe des Fraunhofer ITWM können bezogen werden über:

Fraunhofer-Institut für Techno- und
Wirtschaftsmathematik ITWM
Fraunhofer-Platz 1

67663 Kaiserslautern
Germany

Telefon: 06 31/3 16 00-0
Telefax: 06 31/3 16 00-10 99
E-Mail: info@itwm.fraunhofer.de
Internet: www.itwm.fraunhofer.de

Vorwort

Das Tätigkeitsfeld des Fraunhofer-Instituts für Techno- und Wirtschaftsmathematik ITWM umfasst anwendungsnahe Grundlagenforschung, angewandte Forschung sowie Beratung und kundenspezifische Lösungen auf allen Gebieten, die für Techno- und Wirtschaftsmathematik bedeutsam sind.

In der Reihe »Berichte des Fraunhofer ITWM« soll die Arbeit des Instituts kontinuierlich einer interessierten Öffentlichkeit in Industrie, Wirtschaft und Wissenschaft vorgestellt werden. Durch die enge Verzahnung mit dem Fachbereich Mathematik der Universität Kaiserslautern sowie durch zahlreiche Kooperationen mit internationalen Institutionen und Hochschulen in den Bereichen Ausbildung und Forschung ist ein großes Potenzial für Forschungsberichte vorhanden. In die Berichtreihe sollen sowohl hervorragende Diplom- und Projektarbeiten und Dissertationen als auch Forschungsberichte der Institutsmitarbeiter und Institutsgäste zu aktuellen Fragen der Techno- und Wirtschaftsmathematik aufgenommen werden.

Darüber hinaus bietet die Reihe ein Forum für die Berichterstattung über die zahlreichen Kooperationsprojekte des Instituts mit Partnern aus Industrie und Wirtschaft.

Berichterstattung heißt hier Dokumentation des Transfers aktueller Ergebnisse aus mathematischer Forschungs- und Entwicklungsarbeit in industrielle Anwendungen und Softwareprodukte – und umgekehrt, denn Probleme der Praxis generieren neue interessante mathematische Fragestellungen.

Prof. Dr. Dieter Prätzel-Wolters
Institutsleiter

Kaiserslautern, im Juni 2001

Hierarchy of mathematical models for production processes of technical textiles

Axel Klar* Nicole Marheineke* Raimund Wegener †

April 2009

Abstract: In this work we establish a hierarchy of mathematical models for the numerical simulation of the production process of technical textiles. The models range from highly complex three-dimensional fluid-solid interactions to one-dimensional fiber dynamics with stochastic aerodynamic drag and further to efficiently handable stochastic surrogate models for fiber lay-down. They are theoretically and numerically analyzed and coupled via asymptotic analysis, similarity estimates and parameter identification. The model hierarchy is applicable to a wide range of industrially relevant production processes and enables the optimization, control and design of technical textiles.

Key words: Fiber-fluid interaction, slender-body theory, turbulence modeling, model reduction, stochastic differential equations, Fokker-Planck equation, asymptotic expansions, parameter identification

msc2000: 74F10, 76F60, 41A60, 37H10, 60H30, 65C05

1 Introduction

Technical textiles are nonwoven webs of fibers that find their application in various branches of industry, e.g. in textile, hygiene, automobile and building industry. Typical products are clothing textiles, baby diapers, oil and water filters, sound proofing, insulating material etc. Depending on their use, the textiles have to satisfy certain properties. An important common property for the quality assessment of the fabrics is the homogeneity of the fiber web.

A long-term objective in industry is the optimal design of the production process with respect to the desired product specification. Therefore, it is necessary to model, simulate and control the production process of technical textiles. Of main practical relevance are transversal, rotational and oscillating processes. Differing in details, they have in principal three things in common: spinning, entanglement and lay-down. The individual fibers are obtained by a continuous extrusion of a molten granular through narrow nozzles. Then, they are stretched and entangled by acting turbulent air flows to form a web, while laying down on a moving conveyor belt, figure 1.

In this paper, we present a hierarchy of mathematical models that enables the simulation and control of the production process and even more the prediction and optimization of textile properties, e.g. homogeneity of mass distribution and directional arrangement. The models range from a highly complex three-dimensional fluid-solid problem with slender bodies in turbulent flows to an one-dimensional fiber motion with stochastic aerodynamic drag force and further to an efficiently evaluable stochastic surrogate model for the fiber lay-down. So far, we have analyzed the models separately in theoretical and numerical works. In this paper, we bring them together for the first time. Based on our previously derived results, we couple them using asymptotic analysis, similarity estimates and parameter identification and show their wide range of industrially relevant applications.

The numerical simulations of the spinning and turbulent lay-down regimes in the production processes are performed on the basis of a stochastic generalized string model that is deduced from a Cosserat rod [3] being capable of large, geometrically nonlinear deformations. The interactions of fiber and turbulent flow are thereby incorporated by a stochastic drag force. This force model has been derived on top of a k-ϵ description for the turbulent flow field in [23]. The turbulence effects on the fiber dynamics are modeled by a correlated random Gaussian force and its asymptotic limit on a macroscopic fiber scale by Gaussian white noise with a flow-dependent amplitude that carries the information of kinetic turbulent energy,

*TU Kaiserslautern, Fachbereich Mathematik, Postfach 3049, D-67653 Kaiserslautern
†Fraunhofer ITWM, Fraunhofer Platz 1, D-67663 Kaiserslautern

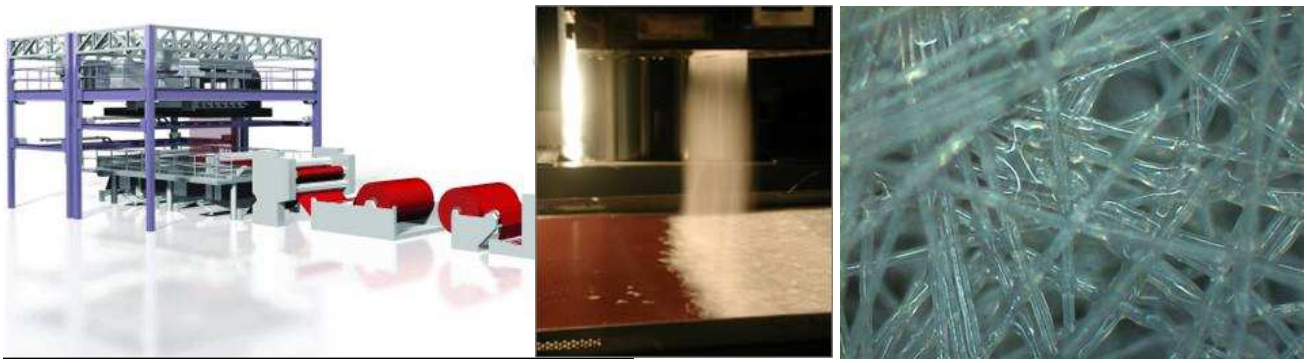

Figure 1: Production of technical textiles. *Left to right:* Plant, laminar lay-down regime, nonwoven material (Photos by Neumag, www.neumag.saurer.com).

dissipation rate and correlation lengths. Numerical studies under the conditions of a production process for technical textiles show good agreement to the experimental observations, see [24] for a non-linear Taylor drag and [25] for a generalized drag model. Due to the huge amount of physical details, the simulations of the fiber spinning and lay-down usually require an extremely large computational effort and high memory storage. This makes the optimization and control of the production process and the product properties very difficult and sometimes even impossible. Since all fibers are realizations of the same stochastic process for the underlying turbulent flow field, we have come up with the idea, [12], to introduce a surrogate stochastic process that do not describe the full dynamics of the fiber, but instead its two-dimensional image on the conveyor belt. Containing parameters that characterize the production process (turbulence influence, buckling behavior, spinning speed, velocity of conveyor belt etc.), this simplified lay-down model of stochastic differential equations can be calibrated by help of a full dynamical simulation for a single fiber. Then, it enables the fast and efficient calculation of thousands of fibers for the nonwoven production. In [12] the associated Fokker-Planck equation and stationary solution are investigated for the case of a non-moving conveyor belt. Without turbulence noise the surrogate model is an Hamiltonian system, for small noise stochastic averaging is applied to derive a stochastic equation for the energy and related functionals of the stochastic process. Ergodicity of the process is proven and explicit rates for the convergence to the stationary solution are obtained in [14]. The assumption of a non-moving conveyor belt is abandoned in [5] where the hydrodynamic (large noise) limit is studied for a transversal production process. Using the method of multiple scales and the Chapman-Enskog method transient and stationary joint probability distributions are determined.

This paper is structured as follows. Starting with the modelling of the fiber dynamics in turbulent flows in section 2, we embed the stochastic generalized string model in the theory of Cosserat rods. Thereby, we pay special attention to the derivation of the stochastic aerodynamic drag force. In section 3 we present the theory for the surrogate stochastic lay-down model. In particular, we generalize the lay-down model so that it shows similar regularity than the string model and is, moreover, applicable to transversal, rotating and oscillating production processes. Section 4 deals with the coupling of the models via an appropriate parameter identification. Using the proposed model hierarchy, we conclude with the simulation of technical textiles and the investigation of production principles for practically relevant processes.

2 Models for fiber dynamics

The description of the fiber dynamics in a flow requires in principal a two-way coupling of fiber and flow with appropriate interface conditions. In case of slender fibers and turbulent flows, the needed high resolution and adaptive grid refinement make the direct numerical simulation of the coupled three-dimensional fluid-solid-problem not only extremely costly and complex, but also mostly impossible for practically relevant applications. Due to the slender geometry the fiber influence on the flow is often negligibly small. Therefore, it makes sense to derive an asymptotic one-dimensional fiber model and to associate to the aerodynamic force a stochastic drag that characterizes the turbulent flow effects on the fiber and enables an one-way coupling.

2.1 Cosserat rod theory

A fiber is a slender long body, i.e. a rod in the context of three-dimensional continuum mechanics, Because of its slender geometry, its dynamics might be reduced to an one-dimensional description by averaging the underlying balance laws over its cross-sections. This procedure is based on the assumption that the displacement field in each cross-section can be

expressed in terms of a finite number of vector- and tensor-valued quantities. The most relevant case is the special Cosserat rod theory that consists of only two constitutive elements, a curve specifying the position and an orthonormal director triad characterizing the orientation of the cross-sections. In the following we introduce the special Cosserat rod theory axiomatically and leave its detailed derivation, justification and generalization to literature [3].

Kinematic and dynamic framework. A special Cosserat rod in the three-dimensional Euclidean space (identified with $\mathbb{R}^3$ via a fixed Cartesian basis) is defined by a curve $\mathbf{r} : (s_a, s_b) \times \mathbb{R} \to \mathbb{R}^3$ and an orthonormal director triad $\{\mathbf{d_1}, \mathbf{d_2}, \mathbf{d_3}\} : (s_a, s_b) \times \mathbb{R} \to \mathbb{R}^3$ where $s \in (s_a, s_b) \subset \mathbb{R}$ denotes a material cross-section (material point) of the rod. The derivatives of the curve $\mathbf{r}$ with respect to time t and material parameter s are the velocity and the tangent field,

$$\mathbf{v} = \partial_t \mathbf{r}, \qquad \boldsymbol{\tau} = \partial_s \mathbf{r}.$$

Due to the orthonormality of the directors there exist vector-valued functions $\boldsymbol{\omega}$ (angular velocity) and $\boldsymbol{\kappa}$ (generalized curvature) satisfying

$$\partial_t \mathbf{d_k} = \boldsymbol{\omega} \times \mathbf{d_k}, \qquad \partial_s \mathbf{d_k} = \boldsymbol{\kappa} \times \mathbf{d_k}$$

for $k = 1, 2, 3$. The definitions of $\mathbf{v}, \boldsymbol{\tau}$ as well as $\boldsymbol{\omega}, \boldsymbol{\kappa}$ imply the compatibility conditions,

$$\partial_t \boldsymbol{\tau} = \partial_s \mathbf{v}, \qquad \partial_t \boldsymbol{\kappa} = \partial_s \boldsymbol{\omega} + \boldsymbol{\omega} \times \boldsymbol{\kappa}.$$

Combing the kinematic equations with the dynamic ones, i.e. the balance laws for linear and angular momentum, yields the full framework of the special Cosserat rod theory

$$\begin{aligned} \partial_t \mathbf{r} &= \mathbf{v}, & \partial_t \mathbf{d_k} &= \boldsymbol{\omega} \times \mathbf{d_k} \\ \partial_t \boldsymbol{\tau} &= \partial_s \mathbf{v}, & \partial_t \boldsymbol{\kappa} &= \partial_s \boldsymbol{\omega} + \boldsymbol{\omega} \times \boldsymbol{\kappa} \\ (\varrho A) \partial_t \mathbf{v} &= \partial_s \mathbf{n} + \mathbf{f}, & \partial_t \mathbf{h} &= \partial_s \mathbf{m} + \boldsymbol{\tau} \times \mathbf{n} + \mathbf{l}. \end{aligned} \tag{1}$$

The line density (ϱA) is defined as Lagrangian quantity in the reference configuration and is hence time-independent. To complete the system, the angular momentum line density $\mathbf{h}$ has to be specified in terms of the kinematic quantities by a geometrical model, the contact force and couple $\mathbf{n}$, $\mathbf{m}$ by material laws and the external loads (body force and body couple line density) $\mathbf{f}$, $\mathbf{l}$ by the considered application.

Remark 2.1 *System* (1) *is formulated in a Lagrangian setting. Alternatively, any other parameterization φ could be chosen. Assuming φ fulfills the initial value problem $\partial_t \varphi(s,t) = u(\varphi(s,t),t)$, $\varphi(s,0) = \varphi_0(s)$. Then, the appropriate re-parameterization of all fields carries convective terms with speed u into system* (1)*. Instead of imposing u, a constraint might be prescribed so that u becomes the associated Lagrangian multiplier and hence an additional unknown of the system. A well-known constraint is the arc-length parameterization of the fiber curve that yields the Eulerian setting.*

For the detailed discussion of closure relations that are useful for production processes of technical textiles we decompose any vector field $\mathbf{x}$ of our rod theory in the director basis $\{\mathbf{d_1}, \mathbf{d_2}, \mathbf{d_3}\}$, i.e. $\mathbf{x} = \sum_{k=1}^{3} x_k \mathbf{d_k}$. Note that the corresponding component triple $\mathsf{x} = (x_1, x_2, x_3)$ in the director basis is strictly to distinguish from the original vector field $\mathbf{x}$ in the fixed Cartesian basis.

Geometric modeling. In general, the angular momentum $\mathbf{h}$ depends linearly on the angular speed $\boldsymbol{\omega}$. To model this functional dependence we need an ansatz how the three-dimensional geometry changes with respect to the deformations of the Cosserat rod. A central role plays the tensor-valued moment of inertia $(\varrho \mathbf{J})(s,t) = (\varrho J)_{ij}(s)\, \mathbf{d_i}(s,t) \otimes \mathbf{d_j}(s,t)$, where the associated matrix $(\varrho \mathsf{J}) = (\varrho J)_{i,j=1,\dots,3}$ is defined in the reference configuration and is hence time-independent. For a homogeneous, circular cross-section of diameter d, we have $(\varrho \mathsf{J}) = (\varrho I)\, \mathrm{diag}(1,1,2)$ with $I = \pi/64 d^4$. Here, we distinguish three geometric models. The easiest one neglects all angular inertia effects, i.e.

$$\mathbf{h} = \mathbf{0}. \tag{2}$$

The resulting degenerated equation $\partial_s \mathbf{m} + \boldsymbol{\tau} \times \mathbf{n} + \mathbf{l} = \mathbf{0}$ might be inserted in the linear momentum equation to simplify the system, see section 2.2. The standard model for elastic Cosserat rods

$$\mathbf{h} = (\varrho \mathbf{J}) \cdot \boldsymbol{\omega}$$

involves the conservation of the cross-sectional shapes under deformation. In contrast, three-dimensional incompressibility leads to shrinking of the cross-sections when stretching the body. This can be described by

$$\mathbf{h} = \frac{1}{\tau_3} (\varrho \mathbf{J}) \cdot \boldsymbol{\omega},$$

see for example [30, 31] modeling a viscous jet.

Material laws. The most important principle for the formulation of material laws for the contact force and couple $\mathbf{n}$, $\mathbf{m}$ is the objectivity, this means the invariance with respect to spatial translation and rotation as well as to time shifts. For this reason, it is most elegant to prescribe the constitutive laws in the director basis $\{\mathbf{d_1}, \mathbf{d_2}, \mathbf{d_3}\}$. We present here two types that are relevant for our application: elastic materials and viscoelastic materials of differential type one. For a general classification we refer to [3]. Constitutive laws are often combined with algebraic constraints restricting the dynamics. Take for example the Kirchhoff constraint $\boldsymbol{\tau} = \mathbf{d_3}$, then $\mathbf{n}$ as Lagrangian multiplier to the constraint becomes a variable of the system (1). The non-extensibility can be weaken by introducing a modified Kirchhoff constraint $\boldsymbol{\tau} = \tau_3 \mathbf{d_3}$, $\tau_3 > 0$. Then, only the normal contact force components n_1 and n_2 are Lagrangian multipliers, whereas the tangential one n_3 together with the contact couple $\mathbf{m}$ have to be specified by a material law.

Elastic materials are generally given by

$$\mathsf{n}(s,t) = \hat{\mathsf{n}}(\tau(s,t), \kappa(s,t), s), \qquad \mathsf{m}(s,t) = \hat{\mathsf{m}}(\tau(s,t), \kappa(s,t), s).$$

For solidified elastic fibers in the production process of technical textiles, the extensibility is negligible. Hence, it makes sense to replace the law for n by the Kirchhoff constraint. Additionally, the linear Bernoulli-Euler law for m might be imposed. For circular cross-sections, we particularly obtain

$$\tau = (0,0,1), \qquad \mathsf{m} = (EI)\,\mathrm{diag}(1,1,(1+\nu_p)^{-1}) \cdot \kappa \tag{3}$$

with Young's modulus E and Poisson number ν_p, see section 2.2 for an application.

Viscoelastic materials of differential type one are generally given by

$$\mathsf{n}(s,t) = \hat{\mathsf{n}}(\tau(s,t), \kappa(s,t), \partial_t\tau(s,t), \partial_t\kappa(s,t), s), \qquad \mathsf{m}(s,t) = \hat{\mathsf{m}}(\tau(s,t), \kappa(s,t), \partial_t\tau(s,t), \partial_t\kappa(s,t), s).$$

For higher differential type, derivatives of higher order are involved consistently. A more general class are viscoelastic materials of type rate equation where n and m satisfy evolution equations. As an example the upper-convective Maxwell (UCM) model or its non-linear generalizations, e.g. the Giesekus model, are used in spinning processes, [13, 20]. For high temperature regions close to the spinning nozzle, the fibers tend to behave like incompressible viscous jets. Then, they are covered by an relation of differential type one with generalized Kirchhoff constraint. For circular cross-sections, we particularly obtain

$$\tau_1 = \tau_2 = 0, \qquad n_3 = 3(\mu A)\,\frac{\partial_t \tau_3}{\tau_3^2}, \qquad \mathsf{m} = 3(\mu I)\,\mathrm{diag}(1,1,2/3) \cdot \frac{\partial_t \kappa}{\tau_3^3}$$

with dynamic viscosity μ of the jet. These constitutive laws are linear in the rates of the strain variables τ, κ, see [30, 31] for their derivation in an Eulerian framework.

External loads. Depending on the considered production process, the external loads $\mathbf{f}$, $\mathbf{l}$ might rise from gravity and / or electromagnetic fields in case of charged fibers. Fiber-wall and fiber-fiber interactions might be incorporated by additional geometrical constraints and associated Lagrangian contact forces. For processes with turbulent lay-down regime, a challenging task is the modelling of the aerodynamic drag that we will discuss in more detail in section 2.2.2. Note that we suppress body couples, $\mathbf{l} = \mathbf{0}$, in the following.

Remark 2.2 *For certain scenarios, asymptotic analysis allows the formally strict derivation of an one-dimensional model. However, the leading-order terms with respect to the slenderness parameter do not result in rod models, but in string models where all angular momentum effects cancel out. They have the form*

$$(\varrho A)\,\partial_{tt}\mathbf{r} = \partial_s\left(N\,\frac{\partial_s \mathbf{r}}{\|\partial_s \mathbf{r}\|}\right) + \mathbf{f},$$

supplemented with a material law for the scalar-valued traction N. For a viscous jet, $N = 3(\mu A)\,\partial_t\|\partial_s\mathbf{r}\|/\|\partial_s\mathbf{r}\|^2$ holds as in the above rod theory, see asymptotic derivation in [25, 28] for curved and [8, 9] for straight viscous fibers in an Eulerian framework.

2.2 Stochastic generalized string model

The Cosserat rod theory allowing for large, geometrically nonlinear deformations enables in principal the numerical simulation of the fiber dynamics in production processes of technical textiles for different materials (viscous, viscoelastic, elastic) and external loads (gravity, electric fields, fiber-wall contacts including friction, fiber-fiber contact, aerodynamic drag forces). But it is still quite complex in this generality. For the resulting properties of the technical textiles the lay-down regime plays an essential role. Thus, focusing on the handling of solidified inextensible elastic fibers in turbulent flows, we introduce an appropriately adapted framework, a so-called stochastic generalized string model.

2.2.1 Embedding into Cosserat rod theory

Restricting to circular cross-sections of diameter d, we consider (1) with the easiest geometric model suppressing angular inertia (2) and the Euler-Bernoulli material law in combination with the Kirchhoff-constraint (3). Then, the angular momentum equation formulated in the director basis reads

$$\partial_s((EI)\kappa_1) - \frac{\nu_p}{1+\nu_p}(EI)\kappa_2\kappa_3 - n_2 = 0, \qquad \partial_s((EI)\kappa_2) + \frac{\nu_p}{1+\nu_p}(EI)\kappa_1\kappa_3 + n_1 = 0, \qquad \partial_s M = 0$$

with torsion couple $M = (EI)\kappa_3/(1+\nu_p)$. Therefore, the contact force $\mathbf{n}$ is determined except of its tangential component $N = n_3$, i.e.

$$\mathbf{n} = \left(-\frac{\nu_p}{1+\nu_p}(EI)\kappa_1\kappa_3 - \partial_s((EI)\kappa_2)\right)\mathbf{d}_1 + \left(-\frac{\nu_p}{1+\nu_p}(EI)\kappa_2\kappa_3 + \partial_s((EI)\kappa_1)\right)\mathbf{d}_2 + N\mathbf{d}_3$$

Using $\partial_s \mathbf{d_k} = \boldsymbol{\kappa} \times \mathbf{d_k}$ and the Kirchhoff constraint we obtain with some calculus

$$\mathbf{n} = T\boldsymbol{\tau} - \partial_s((EI)\partial_s\boldsymbol{\tau}) + M(\boldsymbol{\tau} \times \partial_s\boldsymbol{\tau})$$

where $T = N - (EI)\|\partial_s\boldsymbol{\tau}\|^2$ denotes a generalized tangential contact force. Inserting this relation in system (1), the special Cosserat rod theory reduces to

$$\begin{aligned}
\partial_t \mathbf{r} &= \mathbf{v} \\
\partial_t \boldsymbol{\tau} &= \partial_s \mathbf{v} \\
(\varrho A)\partial_t \mathbf{v} &= \partial_s(T\boldsymbol{\tau} - \partial_s((EI)\partial_s\boldsymbol{\tau})) + M(\boldsymbol{\tau} \times \partial_{ss}\boldsymbol{\tau}) + \mathbf{f}, \qquad \partial_s M = 0 \\
\|\boldsymbol{\tau}\| &= 1.
\end{aligned}$$

Thereby, T acts as Lagrangian multiplier to the inextensibility constraint. Note that we neglect torsion, $M = 0$, which can be justified by appropriate boundary conditions, e.g. a free fiber end. Thus, to simulate the fiber dynamics for the variables $\mathbf{r}, T$, we end up with the following fourth order wavelike system of partial differential equations together with the algebraic constraint of inextensibility,

$$\|\partial_s \mathbf{r}\| = 1, \qquad (\varrho A)\,\partial_{tt}\mathbf{r} = \partial_s(T\partial_s\mathbf{r} - \partial_s((EI)\partial_{ss}\mathbf{r})) + \mathbf{f}, \tag{4}$$

supplemented with appropriate initial and boundary conditions as well as specified external body forces. It has the structure of a string model (remark 2.2), but contains additional bending effects. Hence, we refer to this type of model as generalized string model.

Remark 2.3 *In case of both fiber ends fixed, the directors are prescribed in s_a, s_b. Inserting $\kappa_3 = \mathbf{d_2} \cdot \partial_s \mathbf{d_1}$ in $\partial_s M = 0$, the following boundary value problem has additionally to be solved for each time,*

$$\partial_s\left(\frac{1}{1+\nu_p}(EI)\mathbf{d_2} \cdot \partial_s \mathbf{d_1}\right) = 0, \qquad \mathbf{d_k}(s_a,t) = \mathbf{d}_{\mathbf{k},a}(t), \quad \mathbf{d_k}(s_b,t) = \mathbf{d}_{\mathbf{k},b}(t), \quad k = 1,2$$

yielding the torsion couple M. The directors $\{\mathbf{d_1}, \mathbf{d_2}, \boldsymbol{\tau}\}$ can be expressed in terms of a triad $\{\boldsymbol{\eta_1}, \boldsymbol{\eta_2}, \boldsymbol{\tau}\}$ associated to the curve $\mathbf{r}$ that satisfies the geometrical torsion-free condition $\boldsymbol{\eta_2} \cdot \partial_s \boldsymbol{\eta_1} = 0$ (for an explicit representation see [28]),

$$\mathbf{d_1} = \cos\psi\boldsymbol{\eta_1} + \sin\psi\boldsymbol{\eta_2}, \qquad \mathbf{d_2} = -\sin\psi\boldsymbol{\eta_1} + \cos\psi\boldsymbol{\eta_2},$$

then $\kappa_3 = \partial_s\psi$ holds. This simplifies the boundary value problem to

$$\partial_s\left(\frac{1}{1+\nu_p}(EI)\partial_s\psi\right) = 0, \qquad \psi(s_a,t) = \psi_a(t), \quad \psi(s_b,t) = \psi_b(t),$$

whose solution reads $\psi(s,t) = \psi_a(t) + (\psi_b - \psi_a)(t)\iota(s_a,s)/\iota(s_a,s_b)$ with $\iota(s_a,s) = \int_{s_a}^{s}(1+\nu_p)/(EI)\,\mathrm{d}s'$. Hence,

$$M(s,t) = M(t) = (\psi_b - \psi_a)(t)/\iota(s_a,s_b),$$

where ψ_a and ψ_b have to be computed from the directors and the torsion-free triad at the boundary.

2.2.2 Stochastic drag force

Apart from gravity, the fiber motion in the turbulent lay-down regime is essentially affected by the aerodynamics. To determine the aerodynamic force on the fiber (i.e. the stress on the fiber boundary in outer normal direction), a two-way coupling of fiber and flow with appropriate interface conditions is in general necessary. However, in the asymptotic framework of an one-dimensional generalized string model, we associate to the force a stochastic drag that represents the turbulent flow effects on the fiber and allows an one-way coupling, see [23] for a detailed derivation. Then, system (4) becomes

$$\begin{aligned} \|\partial_s \mathbf{r}\| &= 1, \\ (\varrho A)\, \partial_{tt}\mathbf{r}\, \mathrm{d}s\, \mathrm{d}t &= \{\, \partial_s(T\, \partial_s \mathbf{r} - \partial_s((EI)\, \partial_{ss}\mathbf{r})) + (\varrho A)\, \mathbf{g} + \mathbf{a}(\mathbf{r}, \partial_t \mathbf{r}, \partial_s \mathbf{r}, s, t)\,\}\, \mathrm{d}s\, \mathrm{d}t \\ &\quad + \mathbf{A}(\mathbf{r}, \partial_t \mathbf{r}, \partial_s \mathbf{r}, s, t) \cdot \mathrm{d}\mathbf{w}_{s,t} \end{aligned} \tag{5}$$

with gravity $\mathbf{g}$ and aerodynamics $\mathbf{a}$, $\mathbf{A}$ as external forces, where

$$\begin{aligned} \mathbf{a}(\mathbf{x}, \mathbf{w}, \boldsymbol{\tau}, s, t) &= \mathbf{m}(\boldsymbol{\tau}, \bar{\mathbf{u}}(\mathbf{x}, t) - \mathbf{w}, k(\mathbf{x}, t), \nu(\mathbf{x}, t), \rho(\mathbf{x}, t), d(s)), \\ \mathbf{A}(\mathbf{x}, \mathbf{w}, \boldsymbol{\tau}, s, t) &= \mathbf{L}(\boldsymbol{\tau}, \bar{\mathbf{u}}(\mathbf{x}, t) - \mathbf{w}, k(\mathbf{x}, t), \nu(\mathbf{x}, t), \rho(\mathbf{x}, t), d(s)) \cdot \mathbf{D}(\boldsymbol{\tau}, \bar{\mathbf{u}}(\mathbf{x}, t) - \mathbf{w}, k(\mathbf{x}, t), \varepsilon(\mathbf{x}, t), \nu(\mathbf{x}, t)). \end{aligned}$$

The aerodynamic force is deduced on basis of a stochastic k-ε turbulence model [21]. Expressing the instantaneous flow velocity as sum of a mean and a fluctuating part, the Reynolds-averaged Navier-Stokes equations (RANS) yield a deterministic description for the mean velocity $\bar{\mathbf{u}} : \mathbb{R}^3 \times \mathbb{R}_0^+ \to \mathbb{R}^3$, whereas two further transport equations for the kinetic turbulent energy $k : \mathbb{R}^3 \times \mathbb{R}_0^+ \to \mathbb{R}^+$ and dissipation rate $\varepsilon : \mathbb{R}^3 \times \mathbb{R}_0^+ \to \mathbb{R}^+$ characterize the random fluctuations $\mathbf{u}'$ according to $k = \mathbf{E}[\mathbf{u}' \cdot \mathbf{u}']/2$ and $\varepsilon = \nu\, \mathbf{E}[\nabla \mathbf{u}' : \mathbf{u}']$ with kinematic viscosity ν, density ρ of the air and expectation $\mathbf{E}[.]$. Analogously, the aerodynamic force is split into a mean and a fluctuating part. Acting as additive Gaussian noise in (5), it depends on the flow quantities $\bar{\mathbf{u}}$, k, ε, and ν, ρ. Thereby, the deterministic mean force $\mathbf{m} : \mathbb{R}^2 \times \mathbb{R}^3 \times (\mathbb{R}^+)^4 \to \mathbb{R}^3$ as well as the associated splitting operator $\mathbf{L} : \mathbb{R}^2 \times \mathbb{R}^3 \times (\mathbb{R}^+)^4 \to \mathbb{R}^{3\times 3}$ are essentially determined by the chosen air drag model which is a function of the mean relative velocity between fluid and fiber, $\bar{\mathbf{u}}(\mathbf{r}, t) - \partial_t \mathbf{r}$, and the fiber tangent $\partial_s \mathbf{r}$. The correlated fluctuations are asymptotically approximated by Gaussian white noise with turbulence-dependent amplitude, where $(\mathbf{w}_{s,t}, (s, t) \in (\mathbb{R}_0^+)^2)$ denotes a $\mathbb{R}^3$-valued Wiener process (Brownian motion). The amplitude $\mathbf{D} : \mathbb{R}^2 \times \mathbb{R}^3 \times (\mathbb{R}^+)^3 \to \mathbb{R}^{3\times 3}$ represents the integral effects of the localized centered Gaussian velocity fluctuations on the relevant fiber scales by containing the necessary information of the spatial and temporal correlations of the double-velocity fluctuations. Consequently, the performance of the aerodynamic force mainly relies on two models, i.e. the air drag model (inducing $\mathbf{m}$ and $\mathbf{L}$) and the turbulence correlation approximation (inducing $\mathbf{D}$).

Applying the global-from-local concept of [23], appropriate global models are obtained by superposing local ones. Therefore, we have analyzed, tested and validated experimentally drag models for an incompressible flow around an inclined infinitely long circular cylinder and correlation models for incompressible homogeneous isotropic turbulence in various works [23, 24, 26]. In [24] a nonlinear Taylor drag [33] is applied which is generalized in [26] to fit to all possible flow regimes. The double-velocity correlation tensor has been constructed such that it initially satisfies the Kolmogorov universal equilibrium theory [11] as well as the local distribution of the kinetic energy k and dissipation rate ε provided by the k-ε turbulence model. For its dynamic behavior, Taylor's hypothesis of frozen turbulence pattern [32] originally proposed in [23] and incorporated in [24] is weaken in [26] by prescribing a temporal decay of the local correlations. The latest modifications extend the applicability range of the stochastic force model crucially, see [26] for details and figure 2 for a numerical simulation under industrial conditions.

Remark 2.4 *For mean flows tangentially directed to the fiber and small velocity fluctuations of order ϵ, $\epsilon \ll 1$ (cf. figure 2), existence and uniqueness of a weak solution to* (5) *are proved in [22] for fixed inlet and stress-free fiber end. Expanding the quantities in* (5) *in terms of ϵ, the solution in leading order $\mathbf{r}^{(0)}$, $T^{(0)}$ is the position of rest with the contact force balancing gravity and mean aerodynamic drag force. Using the algebraic constraint yields the vertical position component up to $\mathcal{O}(\epsilon^2)$ and $T^{(1)}$. This reduces one degree of freedom in the evolution equation and halves the number of unknowns. In first order, a linear system of stochastic differential equations for the horizontal components is found which can be embedded in the class of linear wave problems with additive noise. The applicability of the general solution concepts, see [6], is thereby given by the existence of a semigroup and the Hilbert-Schmidt property of the noise amplitude.*

Remark 2.5 *Originally, the aerodynamic force has been modelled as correlated noise due to the underlying correlated flow field, [23]. The transition to the simplified uncorrelated model in* (5) *is only justified for observations on macroscopic fiber scales where the effects of the correlated model on the fiber are very well approximated by the uncorrelated one according to the $\mathcal{L}^2$ and $\mathcal{L}^\infty$-similarity estimates in [23]. These conditions are generally given in industrial production processes of technical textiles as the investigations in [24] show.*

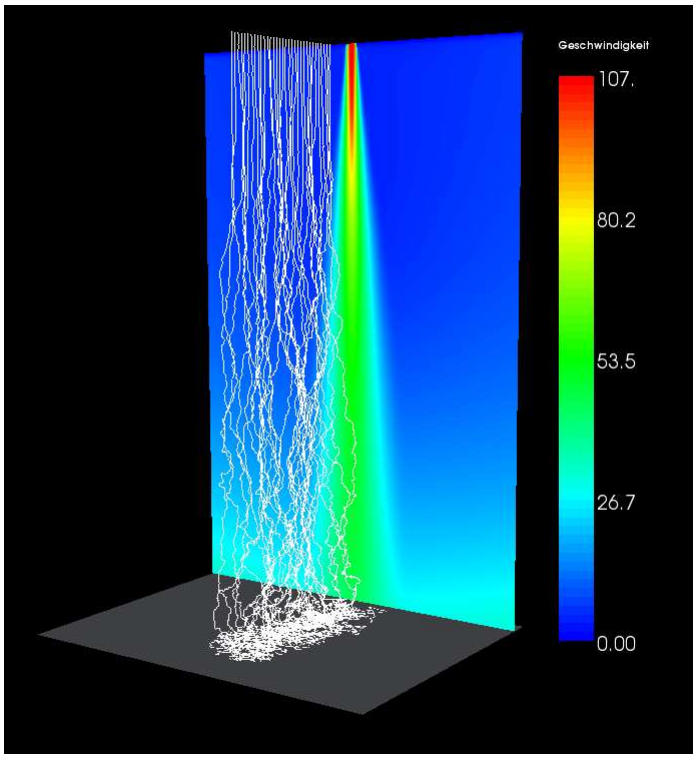

Figure 2: FIDYST simulation of a turbulent lay-down regime: 25 fibers are visualized in white in front of the two-dimensional flow field where the color indicates the magnitude of the mean velocity.

2.2.3 Simulations

The presented stochastic generalized string model for the fiber dynamics is implemented in the software tool FIDYST[1]. Starting with the flow computation, e.g. via commercial tools like FLUENT or CFX, the flow data (mean velocity, kinetic energy, dissipation rate etc.) is handed over to the routine for the fiber dynamics where the nonlinear stochastic system (5) is handled by a method of lines. Thereby, the use of a spatial finite difference method of higher order ensures the appropriate approximation of the algebraic constraint. The Box-Muller method generates the Gaussian deviates for the stochastic drag force. Incorporating the force amplitude on the interpolated flow data explicitly, a semi-implicit Euler method realizes the time integration. Its stability and accuracy is given by an adaptive time step control. The resulting non-linear system of equations is solved by a Newton method. Contact forces due to fiber-wall or fiber-fiber interactions are determined iteratively.

Figure 2 shows a FIDYST simulation for the turbulent lay-down regime of a transversal spinning process as it arises in industrial applications. Thousands of individual endless fibers are spun through narrow nozzles that are densely and equidistantly placed on a row at a spinning beam. The mean flow is homogeneous in direction of the beam and can hence be considered as two-dimensional. The turbulent fluctuations cause the entanglement and loop forming of the fibers that finally lay down on the conveyor belt to form a web. The complexity and effort of the computation and parallelization depend drastically on the number of fibers and the fiber-fiber contacts. In this example, fewer fibers are taken than in reality, moreover the fiber-fiber contacts are neglected. Their deposition on the conveyor belt is realized via a fiber-wall contact with friction such that the fibers finally come to rest, [17]. In spite of these simplifications, the simulation is very time-consuming, storage demanding and not suitable for the production of huge nonwoven webs.

Fortunately, it turns out that this high computational effort is not obligatory. Due to the underlying two-dimensional flow situation, all fibers are realizations of the same stochastic process. Therefore, it makes sense to introduce a simplified surrogate stochastic process that describes the characteristic image of the fibers on the conveyor belt. Containing typical process parameters it might be calibrated by the FIDYST simulation of a single fiber and used for the easy and fast computation of a web of thousands of fibers.

[1] FIDYST: Fiber Dynamics Simulation Tool developed at Fraunhofer ITWM, Kaiserslautern

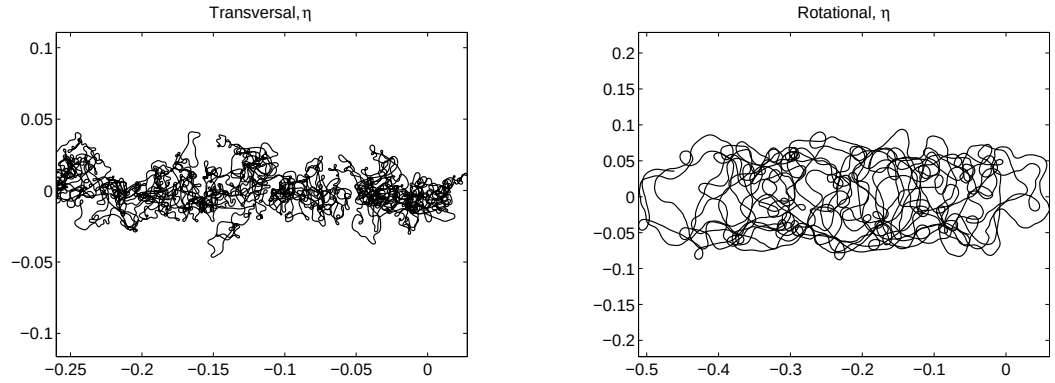

Figure 3: FIDYST simulations of fiber curves $\boldsymbol{\eta}$ for different production processes, transversal and rotational spinning processes.

3 Surrogate stochastic models for fiber lay-down

3.1 Basic model

The idea of the surrogate stochastic models is to describe directly the image of the fiber on the conveyor belt instead of the complex dynamic fiber lay-down process itself. Generalizing the original approach [12], we model this image by help of a stochastic process $(\boldsymbol{\xi}_s, \alpha_s)_{s\in\mathbb{R}_0^+} \in \mathbb{R}^2 \times \mathbb{R}$ where $\boldsymbol{\xi} = \boldsymbol{\eta} - \boldsymbol{\gamma}$ is the difference between the arclength parameterized fiber curve $\boldsymbol{\eta}$ and an idealized reference curve $\boldsymbol{\gamma}$ specifying the production process under consideration and where $\alpha\angle(\mathbf{e_1}, \boldsymbol{\tau})$ is the angle between the production direction $\mathbf{e_1}$ and the tangent $\boldsymbol{\tau}$ on the fiber curve $\boldsymbol{\eta}$, i.e. $\boldsymbol{\tau}(\alpha) = (\cos\alpha, \sin\alpha)$ and $\boldsymbol{\tau}^\perp(\alpha) = (-\sin\alpha, \cos\alpha)$. The process is given by the following system of stochastic differential equations equipped with appropriate initial conditions $\boldsymbol{\xi}_0$, α_0,

$$\mathrm{d}\boldsymbol{\xi}_s = \boldsymbol{\tau}(\alpha_s)\,\mathrm{d}s - \mathrm{d}\boldsymbol{\gamma}_s, \qquad \mathrm{d}\alpha_s = -\nabla B(\boldsymbol{\xi}_s)\cdot\boldsymbol{\tau}^\perp(\alpha_s)\,\mathrm{d}s + A\,\mathrm{d}W_s. \tag{6}$$

The first equation expresses the arclength parameterization of the actual fiber curve $\boldsymbol{\eta}$, whereas the second equation determines the characteristic properties of the lay-down process. Here, the term $-\nabla B(\boldsymbol{\xi})\cdot\boldsymbol{\tau}^\perp(\alpha)$ ensures that $\boldsymbol{\xi}$ is localized around the origin. Hence, the actual fiber curve $\boldsymbol{\eta}$ stays close to the reference curve $\boldsymbol{\gamma}$. A standard model for the buckling behavior is $B(\boldsymbol{\xi}) = (\xi_1^2/\sigma_1^2 + \xi_2^2/\sigma_2^2)/2$ with so-called throwing ranges $\sigma_1, \sigma_2 > 0$. In case of isotropy $B(\boldsymbol{\xi}) = B(\|\boldsymbol{\xi}\|)$, the standard model simplifies to $\sigma_1 = \sigma_2$. The scalar-valued Wiener process $(W_s)_{s\in\mathbb{R}_0^+}$ perturbs the deterministic. Its amplitude $A \geq 0$ contains all random effects of the production process, e.g. the influence of the turbulent flow during the fiber spinning and lay-down, fiber-fiber contacts. Different types of production processes can be described by the appropriate choice of a differentiable reference curve $\boldsymbol{\gamma}$, for example rotational or oscillating spinning processes, figure 3. However, in the following we mainly focus on $\boldsymbol{\gamma}_s = -vs\mathbf{e_1}$, modelling a transversal process with fixed spinning position over a moving conveyor belt. Here, $v = v_{belt}/v_{in} \geq 0$ is the ratio between the belt speed v_{belt} and the typical production speed (fiber length per time) v_{in}, i.e. $v = 0$ holds in case of a non-moving conveyor belt. Fluctuations in the production speed are summarized with all the other random effects in the amplitude A and not explicitly incorporated in the model. The final mass laid down is proportional to the considered fiber length, whenever the fiber has a uniform thickness. For simplicity we restrict to this case. Otherwise (6) might be extended by an additional process describing the thickness fluctuations.

The associated Fokker-Planck equation to (6) for the probability density $p : \mathbb{R}^2\times\mathbb{R}\times\mathbb{R}_0^+ \to \mathbb{R}_0^+$, $(\boldsymbol{\xi}, \alpha, s) \mapsto p(\boldsymbol{\xi}, \alpha, s)$ is given by

$$\partial_s p + \left(\boldsymbol{\tau}(\alpha) + \frac{\mathrm{d}\boldsymbol{\gamma}}{\mathrm{d}s}\right)\cdot\nabla_{\boldsymbol{\xi}} p - \partial_\alpha(\nabla B(\boldsymbol{\xi})\cdot\boldsymbol{\tau}^\perp(\alpha)p) = \frac{A^2}{2}\partial_{\alpha\alpha}p. \tag{7}$$

Remark 3.1 *The stochastic lay-down model* (6) *can be treated as dimensionless with* $\partial_{\xi_1} B(\mathbf{e_1}) = 1$. *This corresponds to a scaled throwing range of order one in belt direction,* $\sigma_1^\star = 1$. *Consequently,* $\sigma_2^\star = \sigma_2/\sigma_1$ *and* $A^\star = \sqrt{\sigma_1}A$. *In case of isotropic buckling, it simplifies to* $B'(1) = 1$ *or* $\sigma_1^\star = \sigma_2^\star = 1$ *respectively, then the noise amplitude* $A^\star$ *characterizes exclusively the relation between stochastic and deterministic rates in the behavior of the system. Dropping* * *we will use the dimensionless form for different investigations in the following, considering linear and quadratic isotropic buckling models, i.e.* $B(\|\boldsymbol{\xi}\|) = \|\boldsymbol{\xi}\|$, $B(\|\boldsymbol{\xi}\|) = \|\boldsymbol{\xi}\|^2/2$.

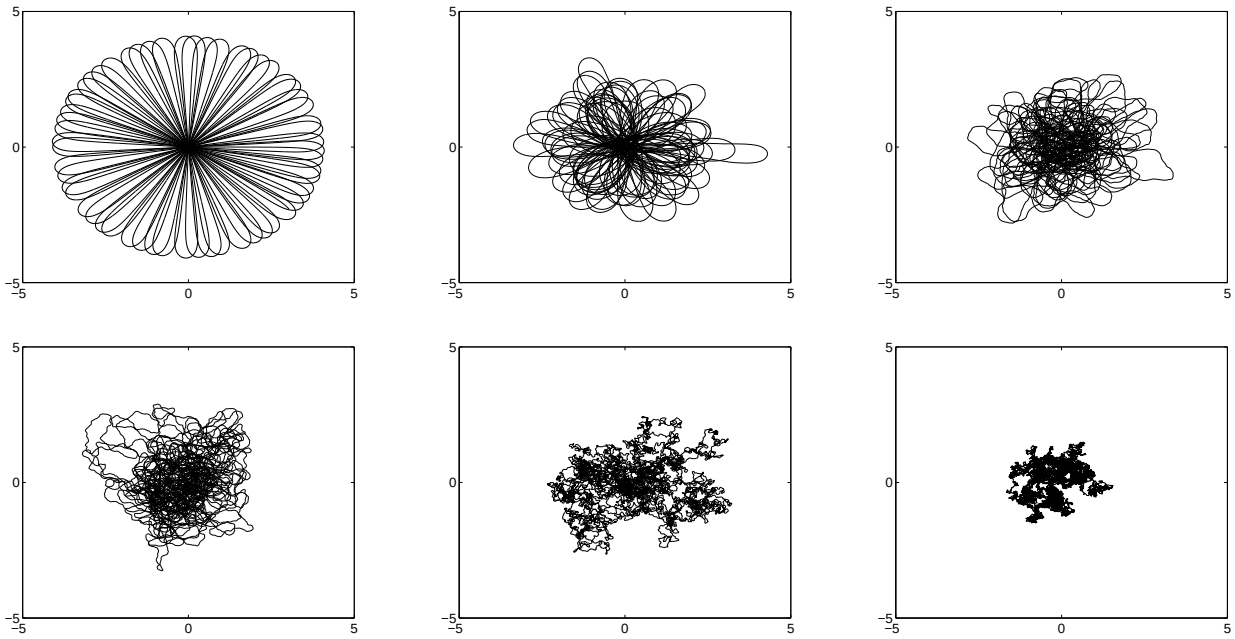

Figure 4: Effect of noise A on fiber trajectory of (8) for isotropic buckling $B(\boldsymbol{\xi}) = \|\boldsymbol{\xi}\|^2/2$. *From left to right, top to bottom*: $A = 0;\ 0.1;\ 1;\ 2;\ 5;\ 10$.

3.1.1 Analysis of special case of a stationary conveyor belt

In this section we restrict to the special case of a non-moving conveyor belt ($v = 0, \boldsymbol{\gamma} \equiv \mathbf{0}$). Then the stochastic system (6) and the associated Fokker-Planck equation (7) simplify to

$$\mathrm{d}\boldsymbol{\xi}_s = \boldsymbol{\tau}(\alpha_s)\,\mathrm{d}s, \qquad \mathrm{d}\alpha_s = -\nabla B(\boldsymbol{\xi}_s)\cdot\boldsymbol{\tau}^{\perp}(\alpha_s)\,\mathrm{d}s + A\,\mathrm{d}W_s. \tag{8}$$

$$\partial_s p + \boldsymbol{\tau}(\alpha)\cdot\nabla_{\boldsymbol{\xi}} p - \partial_\alpha(\nabla B(\boldsymbol{\xi})\cdot\boldsymbol{\tau}^{\perp}(\alpha)p) = \frac{A^2}{2}\partial_{\alpha\alpha} p, \tag{9}$$

respectively. The stationary solution of (9) is independent of α and has particularly the form

$$p_S(\boldsymbol{\xi}) = c\exp(-B(\boldsymbol{\xi})), \quad c > 0 \tag{10}$$

where c is the normalization constant to define the probability measure μ on $\mathbb{R}^2 \times [0, 2\pi]$ having density p_S w.r.t. the Lebesgue measure λ. For the standard buckling model B mentioned above, the stationary distribution p_S is Gaussian with variance matrix $\mathrm{diag}(\sigma_1^2, \sigma_2^2)$ which motivates our used terminology of throwing ranges. For isotropic buckling $B(\|\boldsymbol{\xi}\|) = \|\boldsymbol{\xi}\|^2/2$, the influence of the noise amplitude A on the pathwise behavior of (8) is illustrated in figure 4. In the following, we deal with the approach to equilibrium of the stochastic process, i.e. with the convergence to the stationary solution p_S.

Remark 3.2 *A formal argument for the existence of a global equilibrium, i.e. convergence to the stationary solution* p_S (10)*, comes from the following consideration, cf. [7]. Define the relative entropy*

$$H\left(\frac{p}{p_S}\right) = \int_{\mathbb{R}^2}\int_0^{2\pi} p\ln\left(\frac{p}{p_S}\right)\,\mathrm{d}\alpha\,\mathrm{d}\boldsymbol{\xi}. \tag{11}$$

Then, its temporal change

$$\frac{\mathrm{d}}{\mathrm{d}s}H\left(\frac{p}{p_S}\right) = -\frac{A^2}{2}\int_{\mathbb{R}^2}\int_0^{2\pi} p\left(\partial_\alpha\ln\left(\frac{p}{p_S}\right)\right)^2\,\mathrm{d}\alpha\,\mathrm{d}\boldsymbol{\xi} \le 0$$

can be computed by inserting the Fokker-Planck equation (9)*. Integration by parts together with assumed periodic and decaying boundary conditions in* α *and* $\boldsymbol{\xi}$ *and the fact that* $\boldsymbol{\tau}\cdot\nabla_{\boldsymbol{\xi}} p_S - \partial_\alpha(\nabla B\cdot\boldsymbol{\tau}^{\perp})p_S = 0$ *yields the result above. From the weak monotonicity it might be formally concluded that* p *converges to a local equilibrium determined by* $\mathrm{d}H/\,\mathrm{d}s = 0$.

For arbitrary $A \neq 0$, this stationarity relation holds if and only if the argument is independent of α, hence $p(\boldsymbol{\xi}, \alpha, s) = \rho(\boldsymbol{\xi}, s) p_S(\boldsymbol{\xi})$. Plugging this expression for p into the evolution equation (9) *gives*

$$\partial_s \rho = 0, \qquad \partial_{\xi_1} \rho = 0, \qquad \partial_{\xi_2} \rho = 0$$

because of the linear independence of $\{1, \cos\alpha, \sin\alpha\}$. Due to the normalization condition for the probability densities this means $\rho = 1$. Therefore, we have a global equilibrium $p(\boldsymbol{\xi}, \alpha, s) = p_S(\boldsymbol{\xi})$.

The arguments described in remark 3.2 have been rigorously justified for similar equations in [34]. The application of these methods in the context of the present paper is still an open problem. In the following we choose a different route for a convergence proof and consider the stochastic system (8) directly.

An ergodic result. To prove an ergodic theorem or convergence of the distribution function to a stationary solution, a diffusion process $(\boldsymbol{\xi}_s, \alpha_s)_{s \in \mathbb{R}_0^+}$ solving (8) and having μ as invariant measure is constructed. Let the law of this process be denoted by $\mathbf{P}_\mu$ and the expectation by $\mathbf{E}_\mu[\cdot]$. Then, this diffusion can be shown to be ergodic with rate of convergence

$$\Big\| \frac{1}{s} \int_0^s f(\boldsymbol{\xi}_t, \alpha_t) \, \mathrm{d}t - \mathbf{E}_\mu[f] \Big\|_{\mathcal{L}^2(\mathbf{P}_\mu)} \leq c_1 \Big(\frac{1}{s} + \frac{1}{s^{1/2}} \Big(\frac{c_2}{A} + c_3 A \Big) \Big) \| f - \mathbf{E}_\mu[f] \|_{\mathcal{L}^2(\mu)}, \quad s > 0, \quad (12)$$

with constants $c_i > 0$, $i = 1, 2, 3$ and for arbitrary functions $f \in \mathcal{L}^2(\mu)$, see theorem 3.3 for a rigorous statement and [14] for details. The convergence in (12) implies mean ergodicity of the associated semigroup $(\mathrm{T}_s)_{s \geq 0}$, i.e.

$$\Big\| \frac{1}{s} \int_0^s \mathrm{T}_t f \, \mathrm{d}t - \mathbf{E}_\mu[f] \Big\|_{\mathcal{L}^2(\mu)} \leq c_1 \Big(\frac{1}{s} + \frac{1}{s^{1/2}} \Big(\frac{c_2}{A} + c_3 A \Big) \Big) \| f - \mathbf{E}_\mu[f] \|_{\mathcal{L}^2(\mu)}, \quad s > 0.$$

The generator of this semigroup is

$$\mathrm{L} = \mathrm{L}_1 + \mathrm{L}_2, \quad \text{with } \mathrm{L}_1 = \frac{A^2}{2} \partial_{\alpha\alpha}, \quad \mathrm{L}_2 = \boldsymbol{\tau}(\alpha) \cdot \nabla_{\boldsymbol{\xi}} - \nabla B(\boldsymbol{\xi}) \cdot \tau^\perp(\alpha) \partial_\alpha.$$

Note that the interplay of the operators L_1 and L_2 is crucial for our proof of ergodicity, since L_1 would not cause an ergodic behavior by itself. The idea is to project onto the orthogonal complement of the kernel of $(\mathrm{L}_1, D(\mathrm{L}_1))$. On this subspace, $(\mathrm{L}_1, D(\mathrm{L}_1))$ has a bounded inverse. On the kernel of $(\mathrm{L}_1, D(\mathrm{L}_1))$ in turn, L can be associated with a non-degenerated, self-adjoint operator $(\mathrm{M}, D(\mathrm{M}))$ with

$$\mathrm{M} = \frac{1}{2} \Delta_{\boldsymbol{\xi}} - \frac{1}{2} \nabla B \cdot \nabla_{\boldsymbol{\xi}}$$

in $\mathcal{L}^2(\gamma)$ where γ is the marginal measure of μ on $\mathbb{R}^2$. Assuming that the Dirichlet form $(\mathcal{E}, D(\mathcal{E}))$ corresponding to $(\mathrm{M}, D(\mathrm{M}))$ fulfills a Poincaré inequality, ergodicity can be finally shown. Crucial for the rate of convergence are Kato perturbation techniques and a ground state transform. For the detailed proof we refer to [14].

Theorem 3.3 (Ergodic theorem) *Let $B \in \mathcal{C}^3(\mathbb{R}^2)$, $\nabla B \in \mathcal{L}^2(\gamma)$. Assume that there exist $0 < a < \infty$ and a compact subset $\mathcal{K} \subset \mathbb{R}^2$ such that*

$$(\partial_{\xi_i} \partial_{\xi_j} \partial_{\xi_k} B(\boldsymbol{\xi}))^2 + (\partial_{\xi_i} \partial_{\xi_j} B(\boldsymbol{\xi}))^2 \leq a \big(\partial_{\xi_1} B(\boldsymbol{\xi}) \big)^2 + \big(\partial_{\xi_2} B(\boldsymbol{\xi}) \big)^2 \quad \textit{for all} \quad i, j, k \in \{1, 2\}, \, \boldsymbol{\xi} \in \mathbb{R}^2 \setminus \mathcal{K}.$$

Furthermore, assume that the Dirichlet form $(\mathcal{E}, D(\mathcal{E}))$ fulfills a Poincaré inequality, i.e. there exists $0 < c < \infty$ such that

$$\mathcal{E}(f - \mathbf{E}_\gamma[f], f - \mathbf{E}_\gamma[f]) \geq c \, \big(f - \mathbf{E}_\gamma[f], f - \mathbf{E}_\gamma[f] \big)_{\mathcal{L}^2(\gamma)} \quad \textit{for all} \quad f \in D(\mathcal{E}).$$

Then

$$\Big\| \frac{1}{s} \int_0^s f(\boldsymbol{\xi}_t, \alpha_t) \, \mathrm{d}t - \mathbf{E}_\mu[f] \Big\|_{\mathcal{L}^2(\mathbf{P}_\mu)} \leq \frac{1}{c^{1/2}} \Big(\frac{2}{s} + \frac{1}{s^{1/2}} \Big(\frac{\beta_1(a) c^{1/2} + \beta_2(a) c^{-1/2}}{A} + \Big(1 + \frac{1}{\sqrt{2}} \Big) A \Big) \Big) \| f - \mathbf{E}_\mu[f] \|_{\mathcal{L}^2(\mu)}$$

holds for some constants $0 < \beta_i(a) < \infty$, $i = 1, 2$ independent of a, as well as $f \in \mathcal{L}^2(\mu)$, $A > 0$, and $s > 0$.

Remark 3.4 *The assumptions in theorem 3.3 allow potentials of the form $B(\boldsymbol{\xi}) = \|\boldsymbol{\xi}\|^n$, $n = 2, 4$ or $n \geq 6$, since in these cases a Poincaré inequality holds. More generally, a Poincaré inequality is satisfied, if B grows as fast as or faster than $\|\boldsymbol{\xi}\|$ for large $\boldsymbol{\xi} \in \mathbb{R}^2$.*

Remark 3.5 *Since the adjoint to L w.r.t. the scalar product in $\mathcal{L}^2(\mu)$ is given by $\mathrm{L}^* = \mathrm{L}_1 - \mathrm{L}_2$, we have also ergodicity with the same rate of convergence for the adjoint process and semigroup. Now, strongly mixing of $(\mathrm{T}_s^*)_{s\geq 0}$, i.e. $\lim_{s\to\infty} \|\mathrm{T}_s^* f - \mathbf{E}_\mu[f]\|_{\mathcal{L}^2(\mu)} = 0$, would imply $\mathcal{L}^1$-convergence of the solution p of the associated Fokker-Planck equation* (9) *with normalized non-negative initial distribution $p(0) = p_0$ and Lebesgue measure λ, because*

$$\|p(s) - p_S\|_{\mathcal{L}^1(\lambda)} = \left\| \frac{p(s)}{p_S} - 1 \right\|_{\mathcal{L}^1(\mu)} = \|\mathrm{T}_s^* p_0 - 1\|_{\mathcal{L}^1(\mu)} \leq \|\mathrm{T}_s^* p_0 - 1\|_{\mathcal{L}^2(\mu)}.$$

Since the generator $(\mathrm{L}, D(\mathrm{L}))$ is hypoelliptic in the sense of Hörmander, it is not too hard to show that $(\mathrm{T}_s)_{s\geq 0}$ is strong Feller, [14]. Showing that $(\mathrm{T}_s)_{s\geq 0}$ is additionally irreducible, strongly mixing then follows from Doob's theorem, see e.g. [6]. But we would like to stress that this consideration does not result in an explicit rate of convergence.

Remark 3.6 *It is worth mentioning that the stochastic process associated to the generator M is obtained from the original process* (8) *in the large noise limit, see section 3.1.2.*

Numerical result. To solve the Fokker-Planck equation (9) numerically, a semi-Lagrangian method can be applied, see [18]. This time-splitting method consists of two fractional steps. The first step handles the advection part in a Lagrangian set-up using the modified method of characteristics [10] with adjusted numerical advection to ensure conservation of mass. The second step uses Eulerian coordinates for the discretization of the reaction-diffusion term.

The numerical simulations then allow the investigation of the rate of convergence to the equilibrium p_S w.r.t. an appropriately chosen functional. We focus here on the relative entropy H of (11) which is preferable to other functionals because of its monotonic behavior in s, cf. remark 3.2. Considering the inverse decay rate $\lim_{S\to\infty} \int_0^S H(p(s)/p_S)\,\mathrm{d}s$, figure 5 shows its magnitude for various values of A for linear and quadratic isotropic buckling, $B(\boldsymbol{\xi}) = \|\boldsymbol{\xi}\|$ and $B(\boldsymbol{\xi}) = \|\boldsymbol{\xi}\|^2/2$, S large. Note that the choice of the initial data affects the results quantitatively, but not qualitatively. Hence, a good rate of convergence is found for a finite value of A from the numerical simulations. This observation is confirmed by the analytical estimate in theorem 3.3 according to which the speed of convergence is dominated by the factor $c_1 s^{-1/2}(c_2 A^{-1} + c_3 A)$ with constants c_i, $i = 1, 2, 3$, cf. (12). To this point, figure 4 illustrates representative fibers of same length S and initial data $(\boldsymbol{\xi}_0, \alpha_0)$ that are laid down under quadratic isotropic buckling and the influence of different A. Obviously, the convergence to the stationary standard normal distribution takes longer for very small and large A than for moderate ones, $A \approx 1$.

From a practical point of view, this gives a hint that the process parameters should be adapted in such a way that A is in an intermediate range of values in order to obtain the fastest possible decay to equilibrium and hence a fiber web which is as uniform as possible. However, production processes with non-moving conveyor belt ($v = 0$) are of minor industrial relevance. Hence, we proceed with the investigation of the original lay-down model with moving belt (6).

3.1.2 Investigation of noise influence

The small noise limit. In the following we study the lay-down behavior for small noise $A = \sqrt{\epsilon}A$ and small belt velocity $v = \epsilon v$ on respectively long length scales $s = s/\epsilon$, $0 < \epsilon \ll 1$, restricting to isotropic buckling $B(\boldsymbol{\xi}) = B(\|\boldsymbol{\xi}\|)$ with non-dimensionalizing condition $B'(1) = 1$ (cf. remark 3.1). Stochastic averaging leads hereby to a reduced system for the associated limit energy process as $\epsilon \to 0$ for which the characteristic drift and variance coefficients can be determined.

The stochastic averaging approach is motivated from the fact that the system corresponding to a deterministic lay-down process with non-moving belt, $A = 0$, $v = 0$, is Hamiltonian. In polar coordinates $\boldsymbol{\xi} = r(\cos\phi, \sin\phi)$ and angle $\beta = \alpha - \phi$, it particularly reads

$$\mathrm{d}r_s = \cos\beta_s\,\mathrm{d}s, \quad \mathrm{d}\beta_s = \left(B'(r_s) - \frac{1}{r_s}\right)\sin\beta_s\,\mathrm{d}s, \quad \mathrm{d}\phi_s = \frac{\sin\beta_s}{r_s}\,\mathrm{d}s, \tag{13}$$

with $(r, \beta) \in \mathbb{R}_0^+ \times [0, 2\pi)$. Due to symmetry, the restriction to $\beta \in [0, \pi]$ is sufficient. As illustrated in figure 6, the system moves on closed orbits in the (r, β)-plane with fixpoint $(r, \beta) = (1, \pi/2)$. The periodic orbits are given by the level sets $E(r, \beta) = e \in \mathbb{R}_0^+$ of the Hamiltonian

$$E(r, \beta) = B(r) - \ln r - \ln\sin\beta \tag{14}$$

with $r \in [r_{\min}(e), r_{\max}(e)]$, $0 < r_{\min}(e) < 1 < r_{\max}(e)$ for fixed energy e. The corresponding Hamiltonian coordinates are (r, z) with $z = \ln\tan(\beta/2)$. The period of motion S_E depends generally on the energy, $S_E(e) = \mathrm{d}/\mathrm{d}e(\int_{E(r,z)<e} \mathrm{d}r\mathrm{d}z)$ [12].

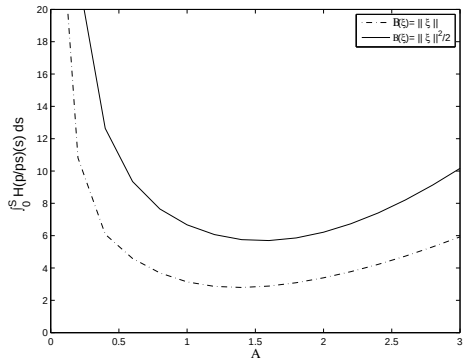

Figure 5: Rates of convergence $\lim_{S\to\infty}\int_0^S H(p(s)/p_S)\,\mathrm{d}s$ for varying noise A, considering linear (-:) and quadratic (–) isotropic B.

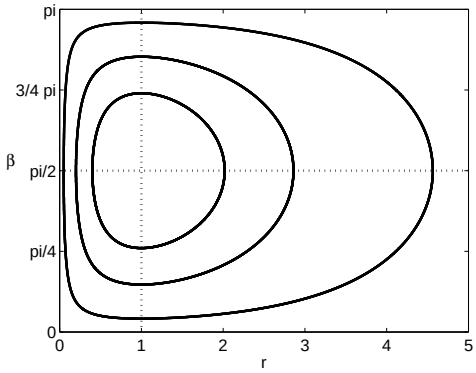

Figure 6: Orbits of the deterministic (r,β)-system in (13) for different energy values e.

Extending (13) to the full lay-down model with small noise $A=\sqrt{\epsilon}A$ and small belt velocity $v=\epsilon v$ on large length scales $s=s/\epsilon$, we obtain a stochastic Hamiltonian system that has the following form for the scaled $(r_s^\epsilon,\beta_s^\epsilon,\phi_s^\epsilon)_{s\in\mathbb{R}_0^+}$-process, $\epsilon\ll 1$,

$$\begin{aligned}
\mathrm{d}r_s^\epsilon &= \left(\frac{1}{\epsilon}\cos\beta_s^\epsilon + v\cos\phi_s^\epsilon\right)\,\mathrm{d}s\\
\mathrm{d}\beta_s^\epsilon &= \left(\frac{1}{\epsilon}\left(B'(r_s^\epsilon)-\frac{1}{r_s^\epsilon}\right)\sin\beta_s^\epsilon + v\frac{\sin\phi_s^\epsilon}{r_s^\epsilon}\right)\,\mathrm{d}s + A\,\mathrm{d}W_s.\\
\mathrm{d}\phi_s^\epsilon &= \left(\frac{1}{\epsilon}\frac{\sin\beta_s^\epsilon}{r_s^\epsilon} - v\frac{\sin\phi_s^\epsilon}{r_s^\epsilon}\right)\,\mathrm{d}s
\end{aligned}$$

or alternatively for the scaled process $(r_s^\epsilon,z_s^\epsilon,\phi_s^\epsilon)_{s\in\mathbb{R}_0^+}$ associated to the Hamiltonian coordinates

$$\begin{aligned}
\mathrm{d}r_s^\epsilon &= \left(-\frac{1}{\epsilon}\frac{\partial}{\partial z}E(r_s^\epsilon,z_s^\epsilon) + v\cos\phi_s^\epsilon\right)\,\mathrm{d}s\\
\mathrm{d}z_s^\epsilon &= \left(\frac{\partial}{\partial r}E(r_s^\epsilon,z_s^\epsilon) + \left(\frac{v\sin\phi_s^\epsilon}{r_s^\epsilon\sin\beta(z_s^\epsilon)} - \frac{A^2\cos\beta(z_s^\epsilon)}{2\sin^2\beta(z_s^\epsilon)}\right)\right)\,\mathrm{d}s + \frac{A}{\sin\beta(z_s^\epsilon)}\,\mathrm{d}W_s\\
\mathrm{d}\phi_s^\epsilon &= \left(\frac{1}{\epsilon}\frac{\sin\beta(z_s^\epsilon)}{r_s^\epsilon} - v\frac{\sin\phi_s^\epsilon}{r_s^\epsilon}\right)\,\mathrm{d}s.
\end{aligned}$$

Following the approach of [12] for the case $v=0$, we introduce the energy process

$$G_s^\epsilon = G(r_s^\epsilon,\beta_s^\epsilon) = \exp(-E(r_s^\epsilon,\beta_s^\epsilon)) = r_s^\epsilon\,\exp(-B(r_s^\epsilon))\,\sin\beta_s^\epsilon,$$

which is a preferable alternative to E of (14) since it is restricted to the interval $[0,1]$. Applying Ito-calculus, we obtain

$$\mathrm{d}G_s^\epsilon = (-\frac{A^2}{2}G_s^\epsilon - vG_s^\epsilon\left(\left(B'(r_s^\epsilon)-\frac{1}{r_s^\epsilon}\right)\cos\phi_s^\epsilon - \frac{1}{r_s^\epsilon}\cot\beta_s^\epsilon\sin\phi_s^\epsilon\right))\,\mathrm{d}s + AG_s^\epsilon\cot\beta_s^\epsilon\,\mathrm{d}W_s.$$

Using the stochastic averaging theorem formally, see e.g. [29] and [1, 2] for an application to stochastic Hamiltonian systems, we determine the limit process G_s^0 for G_s^ϵ, $\epsilon\to 0$, as

$$\mathrm{d}G_s^0 = a(G_s^0)\,\mathrm{d}s + \sigma(G_s^0)\,\mathrm{d}W_s \tag{15}$$

with drift and variance

$$a(g) = -\frac{A^2}{2}g - vg\left\langle\left(B'(r)-\frac{1}{r}\right)\cos\phi - \frac{1}{r}\cot\beta\sin\phi\right\rangle(g),\quad \sigma^2(g) = A^2g^2\,\langle\cot^2\beta\rangle(g)$$

Note that $\langle f\rangle(g) = \int_0^{S_G(g)} f(r_s,\beta_s,\phi_s)\,\mathrm{d}s/S_G(g)$ with period of motion S_G, where (r_s,β_s,ϕ_s) results from the unperturbed motion (13) with energy g. Due to the Riemann-Lebesgue lemma we have

$$-vg\left\langle \left(B'(r)-\frac{1}{r}\right)\cos\phi - \frac{1}{r}\cot\beta\sin\phi\right\rangle(g) = 0$$

such that the drift reduces to $a(g) = -A^2 g/2$. Consequently, the belt velocity v does not influence the averaged equations (15), and the limit energy process coincides with the one obtained for $v = 0$ in [12]. The associated Fokker-Planck equation is

$$\partial_s p + \partial_g(a(g)p) = \frac{1}{2}\,\partial_{gg}(\sigma^2(g)p), \tag{16}$$

complemented with initial data and normalization condition $\int_0^1 p(g,s)\,\mathrm{d}g = 1$. Equipped with appropriate boundary conditions, (16) can be rewritten in the usual form of a Sturm-Liouville problem. For a numerical investigation of the limit process and the distribution of process functionals we refer to [12].

The large noise or hydrodynamic limit. Here, we present the large noise limit that is related to the hydrodynamic limit in kinetic theory. The results are taken from [5]. Here, the lay-down model (6) is considered with large A, scaling $\epsilon = A^{-2} \ll 1$. Then, the associated Fokker-Planck equation (7) for the normalized probability density p, equipped with initial data $p(\boldsymbol{\xi},\alpha,0) = p_0(\boldsymbol{\xi},\alpha)$, reads

$$\partial_s p + (\boldsymbol{\tau}(\alpha) + v\mathbf{e_1})\cdot\nabla_{\boldsymbol{\xi}} p - \partial_\alpha(\boldsymbol{\tau}^\perp(\alpha)\cdot\nabla B(\boldsymbol{\xi})p) = \frac{1}{2\epsilon}\partial_{\alpha\alpha}p. \tag{17}$$

To analyze p and derive a stationary solution in leading order, we apply a Chapman-Enskog type method with the following ansatz

$$p(\boldsymbol{\xi},\alpha,s;\epsilon) = \frac{1}{2\pi}\,\mathcal{P}(\boldsymbol{\xi},s;\epsilon) + \epsilon\, p^{(1)}(\boldsymbol{\xi},\alpha;\mathcal{P}) + \epsilon^2 p^{(2)}(\boldsymbol{\xi},\alpha;\mathcal{P}) + \mathcal{O}(\epsilon^3). \tag{18}$$

where $\mathcal{P}$ is a solution of the leading order problem $\partial_{\alpha\alpha}p = 0$. We anticipate that after a transient in the fast scale $\hat{s} = \epsilon s$ the slowly-varying density $\mathcal{P}$ becomes independent of α, as shown by the method of multiple scales. This certainly ignores an initial layer such that an additional term might be added to account for the effect of initial conditions $p_0(\boldsymbol{\xi},\alpha)$, [5]. The higher order terms $p^{(m)}$, $m = 1,2,\ldots$ are assumed to depend on s only through their dependence on $\mathcal{P}$, and we have

$$\partial_s\mathcal{P} = F^{(0)} + \epsilon F^{(1)} \tag{19}$$

where $F^{(m)}$ are functionals of $\mathcal{P}$ to be determined so that $p^{(m)}$ are bounded and 2π-periodic in α. Inserting (18) and (19) in (17) yields a hierarchy of problems. To ensure that $\mathcal{P}$ contains all the contributions from the homogeneous equations in the hierarchy, we have to impose the additional constraints $\int_{-\pi}^{\pi} p^{(m)}\,\mathrm{d}\alpha = 0$. In $\mathcal{O}(\epsilon)$, we then find

$$\frac{1}{2}\,\partial_{\alpha\alpha}p^{(1)} = F^{(0)} + (\boldsymbol{\tau}(\alpha) + v\mathbf{e_1})\cdot\nabla_{\boldsymbol{\xi}}\mathcal{P} - \partial_\alpha(\boldsymbol{\tau}^\perp(\alpha)\cdot\nabla B(\boldsymbol{\xi})\mathcal{P}), \qquad \int_{-\pi}^{\pi} p^{(1)}\,\mathrm{d}\alpha = 0.$$

The problem has a normalized solution which is 2π-periodic in α, provided the average over one period of the right-hand side of the linear equation vanishes. Hence,

$$0 = F^{(0)} + v\partial_{\xi_1}\mathcal{P}, \tag{20}$$

yielding $F^{(0)}$. This solvability condition implies that the transport of $\mathcal{P}$ with the belt speed v in $\mathbf{e_1}$-direction occurs on the original scale s. Finally, we get

$$p^{(1)} = -2\boldsymbol{\tau}(\alpha)\cdot(\nabla_{\boldsymbol{\xi}} + \nabla B(\boldsymbol{\xi}))\,\mathcal{P}.$$

To determine the remaining term $F^{(1)}$ in the reduced Fokker-Planck equation for $\mathcal{P}$ (19), we proceed with the full problem in $\mathcal{O}(\epsilon^2)$

$$\frac{1}{2}\,\partial_{\alpha\alpha}p^{(2)} = F^{(1)} - 2\boldsymbol{\tau}(\alpha)\cdot(\nabla_{\boldsymbol{\xi}} + \nabla B(\boldsymbol{\xi}))F^{(0)} + (\boldsymbol{\tau}(\alpha) + v\mathbf{e_1})\cdot\nabla_{\boldsymbol{\xi}}p^{(1)} - \partial_\alpha(\boldsymbol{\tau}^\perp(\alpha)\cdot\nabla B(\boldsymbol{\xi})p^{(1)}),$$
$$\int_{-\pi}^{\pi} p^{(2)}\,\mathrm{d}\alpha = 0.$$

The solvability condition, i.e. the average of the right-hand side over one period in α vanishes, gives $F^{(1)}$ analogously,

$$0 = F^{(1)} - \nabla_{\boldsymbol{\xi}} \cdot (\nabla_{\boldsymbol{\xi}} + \nabla B(\boldsymbol{\xi}))\, \mathcal{P}. \tag{21}$$

Inserting the conditions (20) and (21) for $F^{(0)}$ and $F^{(1)}$ in (19) yields the reduced Fokker-Planck equation

$$\partial_s \mathcal{P} = \nabla_{\boldsymbol{\xi}} \cdot (\epsilon \nabla_{\boldsymbol{\xi}} + \epsilon \nabla B(\boldsymbol{\xi}) - v\mathbf{e_1})\, \mathcal{P}$$

with stationary solution

$$\mathcal{P}_S(\boldsymbol{\xi}) = c \exp\left(-B(\boldsymbol{\xi}) - \frac{1}{\epsilon} v \xi_1\right),$$

$c > 0$ normalization constant. The associated stochastic differential equation is

$$\mathrm{d}\boldsymbol{\xi} = (-\epsilon \nabla B(\boldsymbol{\xi}) + v\mathbf{e_1})\, \mathrm{d}s + \sqrt{2\epsilon}\, \mathrm{d}\mathbf{W}_s.$$

The stationary distribution $\mathcal{P}_S$ depends on the noise, as $A = \epsilon^{-1/2}$. This contrasts with the case of a non-moving belt, $v = 0$, in which the stationary distribution is the same for deterministic ($A = 0$) and stochastic ($A > 0$) dynamics, cf. (10). In the hydrodynamic limit $\epsilon \to 0$, $\mathcal{P}_S$ is only independent of ϵ if $v \sim \epsilon$. Then, we deal with lay-down processes of large noise A and small velocity v, where $A \sim v^{-1/2}$.

Remark 3.7 *In this asymptotic regime the fiber lay-down with isotropic buckling $B(\boldsymbol{\xi}) = \|\boldsymbol{\xi}\|^2/2$ is described by the Ornstein-Uhlenbeck process*

$$\mathrm{d}\boldsymbol{\xi} = \left(-\frac{1}{A^2}\boldsymbol{\xi} + v\mathbf{e_1}\right) \mathrm{d}s + \frac{\sqrt{2}}{A}\, \mathrm{d}\mathbf{W}_s, \qquad \partial_s \mathcal{P} = \nabla_{\boldsymbol{\xi}} \cdot \left(\frac{1}{A^2}(\nabla_{\boldsymbol{\xi}} + \boldsymbol{\xi}) - v\mathbf{e_1}\right) \mathcal{P}.$$

Its stationary density distribution is standard Gaussian, centered in $(A^2 v, 0)$.

3.2 Improved smooth model

The basic model (6) gives a continuous fiber curve. To increase the regularity to a continuously differentiable $\boldsymbol{\eta}$, we extend the considered stochastic process to $(\boldsymbol{\xi}_s, \alpha_s, \kappa_s)_{s \in \mathbb{R}_0^+} \in \mathbb{R}^2 \times \mathbb{R} \times \mathbb{R}$ by introducing the curvature κ of $\boldsymbol{\eta}$. Then, the process is modelled by the following system of stochastic differential equations equipped with appropriate initial conditions $\boldsymbol{\xi}_0$, α_0, κ_0,

$$\mathrm{d}\boldsymbol{\xi}_s = \boldsymbol{\tau}(\alpha_s)\, \mathrm{d}s - \mathrm{d}\boldsymbol{\gamma}_s, \qquad \mathrm{d}\alpha_s = \kappa_s\, \mathrm{d}s, \qquad \mathrm{d}\kappa_s = -\frac{1}{R}(\kappa_s + \boldsymbol{\tau}^{\perp}(\alpha_s) \cdot \nabla B(\boldsymbol{\xi}_s))\, \mathrm{d}s + K\, \mathrm{d}W_s. \tag{22}$$

The first two equations yield a differentiable, arclength parameterized fiber curve $\boldsymbol{\eta} = \boldsymbol{\xi} - \boldsymbol{\gamma}$ with curvature κ. The third equation states a relaxation of the curvature to the buckling behavior of the basic model with typical relaxation length $R > 0$ which is perturbed by a Wiener process with amplitude $K \geq 0$.

White noise limit. The improved smooth model (22) has an asymptotic limit to the basic one (6), using an appropriate scaling. The result is well-known in literature [27], it is the white noise limit of the Ornstein-Uhlenbeck process. In particular, we have the scaling

$$R = \epsilon^2 R, \qquad K = \frac{K}{\epsilon^2}, \qquad \kappa = \frac{\kappa}{\epsilon}$$

for (22), yielding the basic model with coefficient $A = RK$ as $\epsilon \to 0$. This can be concluded from the following consideration.

The smooth model accordingly scaled with standard reference curve $\boldsymbol{\gamma}_s = -vs\mathbf{e_1}$ reads

$$\mathrm{d}\boldsymbol{\xi}_s^{\epsilon} = (\boldsymbol{\tau}(\alpha_s^{\epsilon}) + v\mathbf{e_1})\, \mathrm{d}s, \qquad \mathrm{d}\alpha_s^{\epsilon} = \frac{1}{\epsilon}\kappa_s^{\epsilon}\, \mathrm{d}s, \qquad \mathrm{d}\kappa_s^{\epsilon} = -\frac{1}{\epsilon^2 R}(\kappa_s^{\epsilon} + \epsilon \boldsymbol{\tau}^{\perp}(\alpha_s^{\epsilon}) \cdot \nabla B(\boldsymbol{\xi}_s^{\epsilon}))\, \mathrm{d}s + \frac{K}{\epsilon}\, \mathrm{d}W_s.$$

Hereby, the equations for angle and curvature describe a process of Ornstein-Uhlenbeck type, and the scaling is the white noise scaling of the Ornstein-Uhlenbeck process [4, 27]. Considering the associated Fokker-Planck equation

$$\partial_s p^{\epsilon} + (\boldsymbol{\tau}(\alpha) + v\mathbf{e_1}) \cdot \nabla_{\boldsymbol{\xi}} p^{\epsilon} + \frac{1}{\epsilon}\left(\kappa \partial_{\alpha} p^{\epsilon} - \frac{1}{R}(\boldsymbol{\tau}^{\perp}(\alpha) \cdot \nabla B(\boldsymbol{\xi}))\partial_{\kappa} p^{\epsilon}\right) = \frac{1}{\epsilon^2}\left(\frac{1}{R}\partial_{\kappa}(\kappa p^{\epsilon}) + \frac{K^2}{2}\partial_{\kappa\kappa} p^{\epsilon}\right), \tag{23}$$

with decaying boundary conditions in κ, we use a Hilbert expansion for the probability density, $p^\epsilon = p^{(0)} + \epsilon p^{(1)} + \mathcal{O}(\epsilon^2)$, in order to derive the limit equation as $\epsilon \to 0$. In leading order we have

$$\frac{1}{R}\partial_\kappa(\kappa p^{(0)}) + \frac{K^2}{2}\partial_{\kappa\kappa} p^{(0)} = 0.$$

This equation implies that $p^{(0)}$ is Gaussian in the κ-variable. More precisely, defining the integrated probability density $\hat{p}^\epsilon = \int_{\mathbb{R}} p^\epsilon \,\mathrm{d}\kappa$ and particularly $\hat{p}^0 = \int_{\mathbb{R}} p^{(0)} \,\mathrm{d}\kappa$, we can write

$$p^{(0)} = \hat{p}^0(\boldsymbol{\xi}, \alpha)\frac{1}{\sqrt{\pi K^2 R}} \exp\left(-\frac{\kappa^2}{K^2 R}\right).$$

Proceeding with the problem (23) in $\mathcal{O}(\epsilon)$,

$$\kappa\partial_\alpha p^{(0)} - \frac{1}{R}(\boldsymbol{\tau}^\perp(\alpha)\cdot\nabla B(\boldsymbol{\xi}))\partial_\kappa p^{(0)} = \frac{1}{R}\partial_\kappa(\kappa p^{(1)}) + \frac{K^2}{2}\partial_{\kappa\kappa} p^{(1)},$$

there is no explicit expression for $p^{(1)}$. But multiplying the equation with $(-\kappa)$ and integrating over κ gives

$$-\frac{K^2 R}{2}\partial_\alpha \hat{p}^0 - \frac{1}{R}(\boldsymbol{\tau}^\perp(\alpha)\cdot\nabla B(\boldsymbol{\xi}))\hat{p}^0 = \frac{1}{R}\int_{\mathbb{R}} \kappa p^{(1)} \,\mathrm{d}\kappa.$$

Considering now the integrated Fokker-Planck equation (23)

$$\partial_s \hat{p}^\epsilon + (\boldsymbol{\tau}(\alpha) + v\mathbf{e_1})\cdot\nabla_{\boldsymbol{\xi}}\hat{p}^\epsilon + \frac{1}{\epsilon}\partial_\alpha \int_{\mathbb{R}} \kappa p^\epsilon \,\mathrm{d}\kappa = 0,$$

the integral can be expressed in terms of $\hat{p}^0$ by help of the previous results

$$\int_{\mathbb{R}} \kappa p^\epsilon \,\mathrm{d}\kappa = \int_{\mathbb{R}} \kappa(p^{(0)} + \epsilon p^{(1)})\,\mathrm{d}\kappa + \mathcal{O}(\epsilon^2) = -\epsilon\left(\boldsymbol{\tau}^\perp(\alpha)\cdot\nabla B(\boldsymbol{\xi})\hat{p}^0 + \frac{K^2R^2}{2}\partial_\alpha \hat{p}^0\right) + \mathcal{O}(\epsilon^2).$$

Hence, in the limit $\epsilon \to 0$ we recover the Fokker-Planck equation (7) associated to the basic lay-down model with $A = RK$,

$$\partial_s \hat{p}^0 + (\boldsymbol{\tau}(\alpha) + v\mathbf{e_1})\cdot\nabla_{\boldsymbol{\xi}}\hat{p}^0 - \partial_\alpha(\boldsymbol{\tau}^\perp(\alpha)\cdot\nabla B(\boldsymbol{\xi})\hat{p}^0) = \frac{K^2R^2}{2}\partial_{\alpha\alpha}\hat{p}^0.$$

Influence of parameters. Studying the smooth model numerically, we focus on the influence of two parameters, the relaxation length R and the noise amplitude $RK = A$. Therefore, we restrict to isotropic quadratic buckling and non-moving conveyor belt in the simulation. Figure 7 visualizes the effects of small and large R and A on the fiber trajectory. As in the basic model, the noise amplitude A determines the curling behavior and the size of formed loops: the higher A is, the finer is the entanglement. The relaxation length R in contrast is a measure for the steadiness of the fiber curve. For small relaxation length R the curve is qualitatively similar to those obtained from the basic model (see figure 4), whereas for larger R, it becomes more steady. For further numerical investigations and the derivation of the hydrodynamic limit for the smooth model analogously to section 3.1.2, we refer to [15].

4 Modelling and simulation of technical textiles

An efficient numerical handling of the complete production process of technical textiles requires the coupling of the stochastic generalized string model for the fiber dynamics with a surrogate stochastic model for the fiber lay-down, see sections 2 and 3, respectively. Hereby, we restrict to a FIDYST simulation of a single representative fiber and adjust then the parameters of the simple surrogate lay-down model so that the resulting fiber path coincides qualitatively and quantitatively well with the one given by the complex string model. The subsequent run of the surrogate model allows the cheap and fast simulation of thousands of fibers, yielding the desired fiber web.

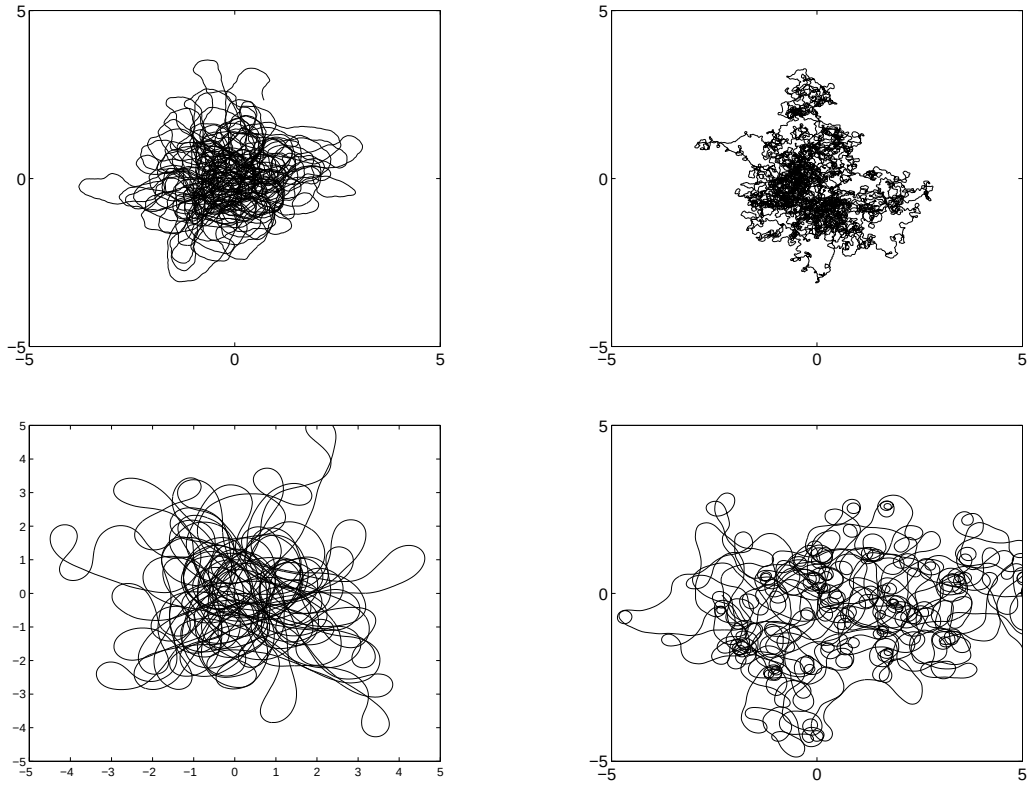

Figure 7: Effect of relaxation length R and noise RK on trajectories of smooth model (22) for $v = 0$ and $B(\boldsymbol{\xi}) = \|\boldsymbol{\xi}\|^2/2$ (cf. figure 4). *Top to bottom*: $R = 10^{-4}$; 1. *Left to right*: $RK = 1$; 5.

4.1 Parameter identification

The performance of the mentioned model reduction depends essentially on the parameter estimation. See for example [19] for the estimation of parametric diffusion models given by stochastic differential equations. Here, we apply a heuristic method to identify the parameters. It turns out to be very stable and efficient in a wide range of applications. In case of a fixed spinning position over a moving conveyor-belt (transversal spinning process), the reference curve $\boldsymbol{\gamma}_s = -vs\mathbf{e_1}$ is prescribed by the speed ratio $v = v_{belt}/v_{in}$. For rotational spinning processes with angle speed ω_{rot}, cycloids form out $\boldsymbol{\gamma}_s = -vs\mathbf{e_1} + r(\cos(\omega s + \phi), \sin(\omega s + \phi))$. Hereby, $\omega = \omega_{rot}/v_{in}$ as well as v are given process parameters, whereas the typical radius r and phase shift ϕ have to be identified, e.g. by the best parametric fit to the fiber curve $\boldsymbol{\eta}$. For completeness, $\boldsymbol{\gamma}_s = -vs\mathbf{e_1} + r\sin(\omega s + \phi)\mathbf{e_2}$ is the reference curve of a spinning process with oscillations normal to the conveyor belt. In the following, we assume that $\boldsymbol{\gamma}$ is known and $\boldsymbol{\xi} = \boldsymbol{\eta} - \boldsymbol{\gamma}$ is centered in the origin. Moreover, motivated by the dynamical simulations, we focus on the standard buckling behavior $B(\boldsymbol{\xi}) = (\xi_1^2/\sigma_1^2 + \xi_2^2/\sigma_2^2)/2$.

Considering a sample of N equidistantly chosen fiber points with associated angle and curvature values $\boldsymbol{D} = (\mathbf{D_1}, ..., \mathbf{D_N}) \in (\mathbb{R}^2 \times \mathbb{R} \times \mathbb{R})^N$, $\mathbf{D_i} = (\boldsymbol{\xi}_i, \alpha_i, \kappa_i) = (\boldsymbol{\xi}_{s_i}, \alpha_{s_i}, \kappa_{s_i})$ and $s_{i+1} - s_i = \triangle s$ fixed, we define a functional of characteristic process properties as

$$\boldsymbol{\mathcal{F}}(\boldsymbol{D}) = \left(\sqrt{\frac{\sum_{i=1}^N \xi_{i,1}^2}{N}}, \sqrt{\frac{\sum_{i=1}^N \xi_{i,2}^2}{N}}, \max_k \sqrt{\frac{\sum_{i=1}^{N-k} (\alpha_{i+k} - \alpha_i)^2}{k\triangle s(N-k)}}, \max_k \sqrt{\frac{\sum_{i=1}^{N-k} (\kappa_{i+k} - \kappa_i)^2}{k\triangle s(N-k)}} \right) \tag{24}$$

with $k = 1, 2, ..., k_{max}$ and $k_{max} \ll N$. To estimate the parameters $\mathbf{P} = (\sigma_1, \sigma_2, RK, K)$ of the surrogate model (22) for a certain production process, we evaluate a FIDYST simulation and set up a respective data sample $\boldsymbol{D}_{fidyst}$ where angle and curvature values are approximated by help of finite differences from the discrete $\boldsymbol{\xi}_i$, $i = 1, ..., N$. The best approximation of the desired quantity $\boldsymbol{\mathcal{F}}(\boldsymbol{D}_{fidyst}) = \mathbf{F}$ are obtained by the surrogate model $\boldsymbol{D}_{sur}$ for the parameters $\mathbf{P}^\star$,

$$\mathbf{P}^\star = \mathrm{argmin}_{\mathbf{P} \in (\mathbb{R}_0^+)^4} \|\boldsymbol{\mathcal{F}}(\boldsymbol{D}_{sur}(\mathbf{P})) - \mathbf{F}\|_2^2.$$

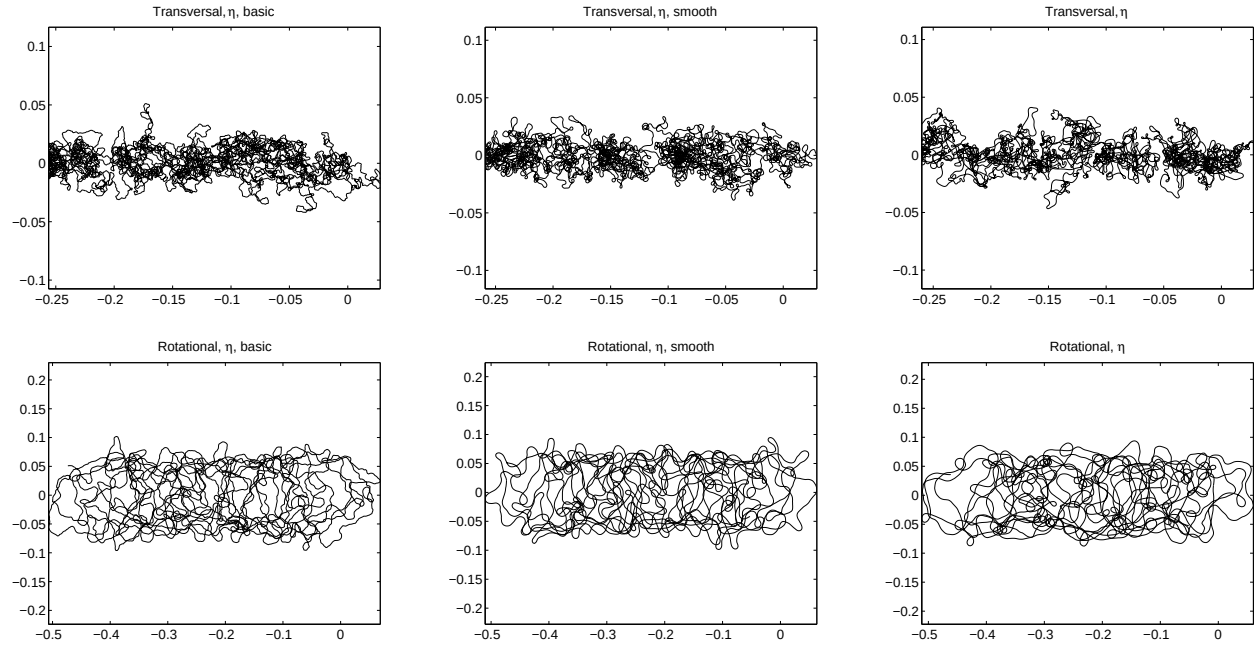

Figure 8: Comparison of fiber curves associated to the surrogate lay-down models (*left:* basic, *middle:* improved smooth) and the FIDYST simulation (*right*) for transversal and rotating spinning processes (cf. figure 3).

To solve this minimization problem, we use a relaxated quasi Newton method with unit Jacobian, $\mathbf{P}^{(j+1)} = \mathbf{P}^{(j)} + \omega(\mathbf{F} - \boldsymbol{\mathcal{F}}(\boldsymbol{D}_{sur}(\mathbf{P}^{(j)}))$, $\omega > 0$ and initial guess $\mathbf{P}^{(0)} = \mathbf{F}$. The convincing performance of this approach results from the fact that the functional $\boldsymbol{\mathcal{F}}$ is a very good estimator for the process parameters $\mathbf{P}$. It is even perfect for σ_1 and σ_2 in the case $\boldsymbol{\gamma} = \mathbf{0}$, for RK in the white noise limit ($RK = A$ see section 3.2) and for the noise amplitude K in general.

Remark 4.1 *To identify the parameters* $\mathbf{P} = (\sigma_1, \sigma_2, A)$ *for the basic surrogate model* (6) *we apply the same strategy as above, but consider a reduced functional containing only the first three components of* $\boldsymbol{\mathcal{F}}$ *in* (24)*. The curvature* κ *is not defined in* (6)*.*

We apply the parameter identification to transversal and rotational spinning processes. Figure 8 shows fiber trajectories associated to the basic and improved lay-down model, respectively, in comparison to the underlying FIDYST realization. Qualitatively, both lay-down models yield a reasonable distribution of the fiber mass. But the behavior of the curvature is certainly better approximated by the improved smooth one. To come to a more quantitative validation of the surrogate models, we consider the variance of the increments of angle and curvature, more precisely

$$\Gamma_\alpha(h) = \frac{1}{\sqrt{h}}\sqrt{\mathbf{E}[(\alpha_{s+h} - \alpha_s)^2]}, \qquad \Gamma_\kappa(h) = \frac{1}{\sqrt{h}}\sqrt{\mathbf{E}[(\kappa_{s+h} - \kappa_s)^2]}.$$

Those maxima enter the functional $\boldsymbol{\mathcal{F}}$ (24) in a discretized version ($h = k\triangle s$), presupposing ergodicity of the processes. Figure 9 illustrates the run of Γ_α, Γ_κ for FIDYST and the smooth improved model as well as of Γ_α for the basic one. According to the identification strategy the basic model gives the same maximum as the FIDYST data. Moreover, it shows the correct decaying behavior. The increase for small h cannot be achieved due to the lack of differentiability. The improved smooth model overcomes this drawback and gives even more the correct decaying behavior in Γ_κ, yielding a coinciding entanglement structure.

4.2 Virtual technical textiles

The calibrated surrogate models for fiber lay-down enable the simulation of technical textiles by superposing thousands of spinning positions. The effects of fiber-fiber interactions are thereby contained in the stochastics of the lay-down. The homogeneity and load capacity of the resulting fiber web are the most important textile properties for the quality assessment of industrial nonwoven fabrics. They are essentially determined by the distribution of fiber mass and directional arrangement in the web which can be studied numerically via Monte-Carlo simulations and validated with experimental data.

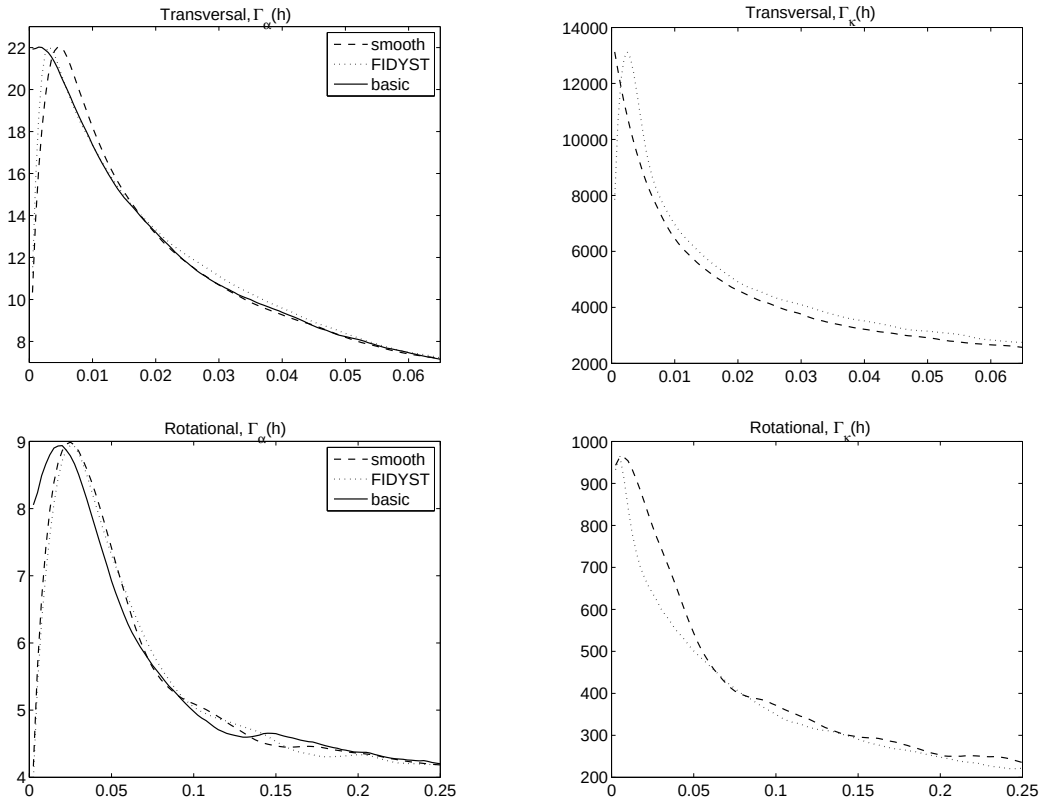

Figure 9: Comparison of Γ_α and Γ_κ for the data in figure 8.

Figure 10 illustrates technical textiles for a transversal spinning process, $\boldsymbol{\gamma}_s = -vs\mathbf{e_1}$, computed with a calibrated smooth lay-down model. The homogeneity of the fiber web is ensured by moderate noise $RK = A$ and small speed ratio v according to the investigations in section 3.1.2, presupposing an appropriate relation, e.g. $d < \sigma_2$, between the distance d of neighboring spinning positions and σ_2. The fiber throwing range σ_1 plays a minor role in the mass distribution. This is not the case for rotational and oscillating spinning processes. Here, the reference curve

$$\boldsymbol{\gamma}_s = -vs\mathbf{e_1} + (r_1\cos(\omega s + \phi), r_2\sin(\omega s + \phi))$$

with $r_1 = r_2$ or $r_1 = 0$ respectively – in particular the interplay between v and ω – determines crucially the fiber web. For given noise, speed ratio and buckling, already slight changes of the angle speed ratio ω might cause the transition from an homogeneous web to one with a characteristic deterministic pattern of undesired strips and holes, see figure 11.

To improve the quality of the industrial fabrics we might apply a technical optimization on the proposed model hierarchy. Changing parameters of the plant or conditions of the production process (e.g. turbulent behavior of the flow acting on the fibers, dynamics of the spinning positions, inflow velocity of the fibers), we firstly evaluate a k-ϵ turbulence simulation for the fluid flow to compute then the dynamics of a single fiber with the stochastic generalized string model. From the result we identify the input parameters for the stochastic lay-down model which we use for the simulation of a fiber web. The parameters and properties of the produced material determine finally the new quality. Apart from these optimization and control aspects, the model hierarchy allows furthermore the numerical investigation of production principles which might result in innovative, efficient and cheap design of new products, for an industrial application we refer to [16].

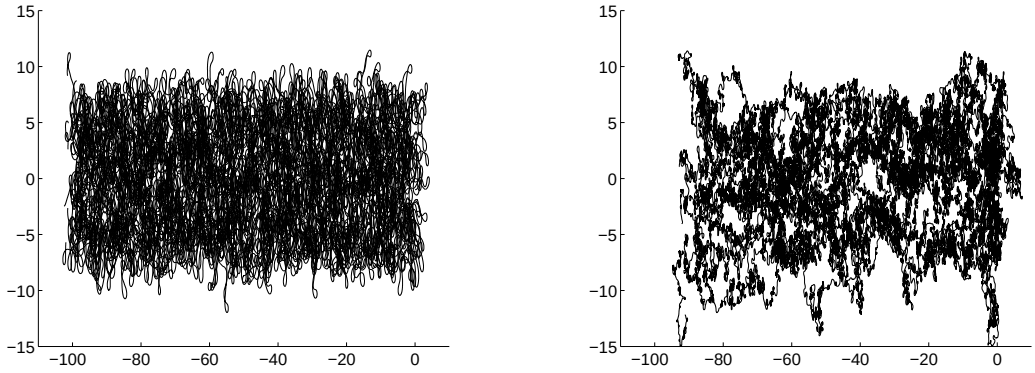

Figure 10: Nonwovens of a transversal spinning process ($\sigma_1 = \sigma_2 = R = 1$, $v = 0.1$) for different noise. *Left:* $RK = 1$. *Right:* $RK = 10$.

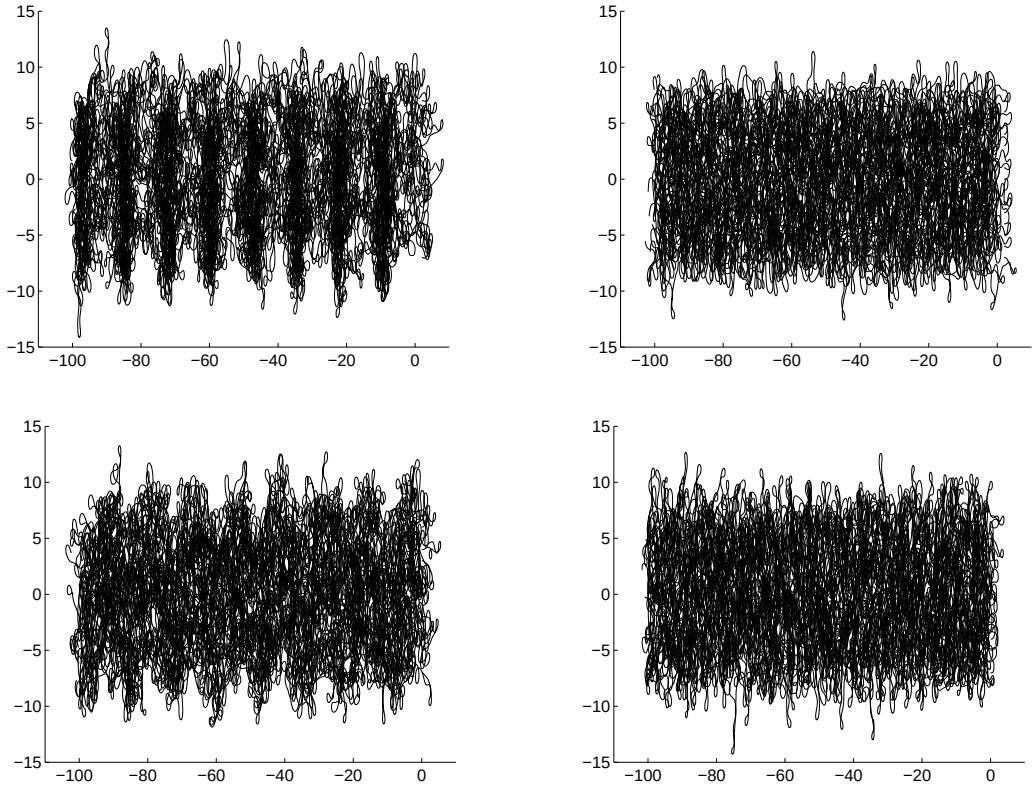

Figure 11: Lay-down principles for rotational (*top*, $r_1 = r_2 = 2$) and oscillating spinning processes (*bottom*, $r_1 = 0$, $r_2 = 2$) with the same parameters as in figure 10 and fixed noise $RK = 1$. *Left:* $\omega = 0.05$. *Right:* $\omega = 0.5$.

5 Conclusion and outlook

In this work we have established a hierarchy of mathematical models for the simulation of the complete production process of technical textiles. The models of different complexity – ranging from highly complex three-dimensional fluid-solid interactions to one-dimensional fiber dynamics with stochastic drag and further to simpler, efficiently handable stochastic fiber lay-down models – are coupled via asymptotic analysis, similarity estimates, parameter identification and validated with experimental data. Applicable to a wide range of practically relevant processes, the model hierarchy has already been used successfully for optimization, control and design of technical textiles in projects with industry.

A long-term objective is the handling of the complete engineering for technical textiles including production process,

micro-structure and product simulation. This requires the expansion of our model chain to the product by integrating micro-structure simulation and design. Our final, industrially motivated goal is the optimal design of the production process with respect to the desired product specification. But by then a lot of interesting mathematical challenges have to be tackled.

Acknowledgement We would like to acknowledge our colleagues with whom these results have been obtained, in particular Thomas Götz, Martin Grothaus, Luis L. Bonilla, Sebastien Motsch and Mohammed Seaid. Moreover, our special thanks go to our colleagues Sergey Antonov, Robert Feßler, Dietmar Hietel and Ferdinand Olawsky at Fraunhofer ITWM, Department Transport Processes, who are developing models, algorithms and software for fiber dynamics in the mentioned production processes, especially the used Fiber Dynamics Simulation Tool (FIDYST). This work has been supported by Rheinland-Pfalz Excellence Center for Mathematical and Computational Modeling $(CM)^2$ and by Deutsche Forschungsgemeinschaft (DFG), WE 2003/3-1, KL 1105/18-1.

References

[1] S. ALBEVERIO and A. KLAR, Longtime behaviour of nonlinear stochastic oscillators, J. Math. Phys. **35**(8), 4005–4027 (1994).

[2] S. ALBEVERIO and A. KLAR, Longtime behaviour of stochastic Hamiltonian systems, Potential Analysis **12**, 281–297 (2000).

[3] S. S. ANTMAN, Nonlinear Problems of Elasticity (Springer Verlag, New York, 2006).

[4] L. ARNOLD, Stochastic Differential Equations (Springer, New York, 1978).

[5] L. L. BONILLA, T. GÖTZ, A. KLAR, N. MARHEINEKE, and R. WEGENER, Hydrodynamic limit for the Fokker-Planck equation describing fiber lay-down models, SIAM J. Appl. Math. **68**(3), 648–665 (2007).

[6] G. DA PRATO and J. ZABCZYK, Stochastic Equations in Infinite Dimensions (Cambridge Unversity Press, 1992).

[7] L. DESVILETTES and C. VILLANI, On the trend to global equilibrium for spatially inhomogeneous entropy-dissipating systems: The linear Fokker-Planck equation, Comm. Pure Appl. Math. **54**, 1–42 (2001).

[8] J. N. DEWYNNE, P. D. HOWELL, and P. WILMOTT, Slender viscous fibers with inertia and gravity, Quart. J. Mech. Appl. Math. **47**, 541–555 (1994).

[9] J. N. DEWYNNE, J. R. OCKENDON, and P. WILMOTT, A systematic derivation of the leading-order equations for extensional flows in slender geometries, J. Fluid Mech. **244**, 323–338 (1992).

[10] J. DOUGLAS, C. HUANG, and F. PEREIRA, The modified method of characteristics with adjusted advection, Numer. Math. **83**, 353–369 (1999).

[11] U. FRISCH, Turbulence. The Legacy of A. N. Kolmogorov (Cambridge University Press, 1995).

[12] T. GÖTZ, A. KLAR, N. MARHEINEKE, and R. WEGENER, A stochastic model and associated Fokker-Planck equation for the fiber lay-down process in nonwoven production processes, SIAM J. Appl. Math. **67**(6), 1704–1717 (2007).

[13] Z. GOU and A. J. MCHUGH, A comparison of Newtonian and viscoelastic constitutive models for dry spinning of polymer fibers, J. Appl. Poly. Sci. **87**(13), 2136–2145 (2003).

[14] M. GROTHAUS and A. KLAR, Ergodicity and rate of convergence for a non-sectorial fiber lay-down process, SIAM J. Math. Anal. **40**(3), 968–983 (2008).

[15] M. HERTY, A. KLAR, S. MOTSCH, and F. OLAWSKY, Smooth stochastic model for fiber lay-down, Preprint (2009).

[16] D. HIETEL, M. GÜNTHER, and F. OLAWSKY, Technologiesprung durch Simulation von Fadendynamiken, Proceeding Hofer Vliesstofftage (2008).

[17] D. HIETEL and R. WEGENER, Simulation of spinning and laydown processes, Technical Textiles **3**, 145–148 (2005).

[18] A. KLAR, P. REUTERSWAERD, and M. SEAID, A semi-Lagrangian method for a Fokker-Planck equation describing fibre dynamics, J. Sci. Comp. **38**(3), 349–367 (2009).

[19] Y. KUTOYANTS, Statistical Inference for Ergodic Diffusion Processes (Springer, London, 2004).

[20] R. G. LARSON, Instabilities in viscoelastic flows, Rheol. Acta **31**, 213–263 (1992).

[21] B. E. LAUNDER and B. I. SHARMA, Application of the energy dissipation model of turbulence to the calculation of flow near a spinning disc, Letters in Heat and Mass Transfer **1**(2), 131–138 (1974).

[22] N. MARHEINEKE, Existence result for a stochastic partial differential algebraic system, Preprint (2009).

[23] N. MARHEINEKE and R. WEGENER, Fiber dynamics in turbulent flows: General modeling framework, SIAM J. Appl. Math. **66**(5), 1703–1726 (2006).

[24] N. MARHEINEKE and R. WEGENER, Fiber dynamics in turbulent flows: Specific Taylor drag, SIAM J. Appl. Math. **68**(1), 1–23 (2007).

[25] N. MARHEINEKE and R. WEGENER, Asymptotic model for the dynamics of curved viscous fibers with surface tension, J. Fluid Mech. **622**, 345–369 (2009).

[26] N. MARHEINEKE and R. WEGENER, Modeling and validation of a stochastic drag for fiber dynamics in turbulent flows, Preprint (2009).

[27] E. NELSON, Dynamical theories of Brownian motion (Princeton University Press, 1967).

[28] S. PANDA, N. MARHEINEKE, and R. WEGENER, Systematic derivation of an asymptotic model for the dynamics of curved viscous fibers, Math. Meth. Appl. Sci. **31**, 1153–1173 (2008).

[29] G. PAPANICOLAOU, D. STROOCK, and S. VARADHAN, Martingale approach to some limit theorems, in: Statistical Mechanics and Dynamical Systems, edited by D. Ruelle (Dueke University Mathematics Series III, Durham, 1978).

[30] N. M. RIBE, Coiling of viscous jets, Proc. Roy. Soc. London, A **2051**, 3223–3239 (2004).

[31] N. M. RIBE, M. HABIBI, and D. BONN, Stability of liquid rope coiling, Phys Fluids **18**, 084102 (2006).

[32] G. I. TAYLOR, The spectrum of turbulence, Proc. Roy. Soc. London, A **164**, 476–490 (1938).

[33] G. I. TAYLOR, Analysis of the swimming of long and narrow animals, Proc. Roy. Soc. London, A **214**, 158–183 (1952).

[34] C. VILLANI, Hypocoercivity, Preprint (arxiv.org/abs/math.AP/0609050) (2006).

Published reports of the Fraunhofer ITWM

The PDF-files of the following reports are available under:
www.itwm.fraunhofer.de/de/zentral__berichte/berichte

1. D. Hietel, K. Steiner, J. Struckmeier
A Finite - Volume Particle Method for Compressible Flows
(19 pages, 1998)

2. M. Feldmann, S. Seibold
Damage Diagnosis of Rotors: Application of Hilbert Transform and Multi-Hypothesis Testing
Keywords: Hilbert transform, damage diagnosis, Kalman filtering, non-linear dynamics
(23 pages, 1998)

3. Y. Ben-Haim, S. Seibold
Robust Reliability of Diagnostic Multi-Hypothesis Algorithms: Application to Rotating Machinery
Keywords: Robust reliability, convex models, Kalman filtering, multi-hypothesis diagnosis, rotating machinery, crack diagnosis
(24 pages, 1998)

4. F.-Th. Lentes, N. Siedow
Three-dimensional Radiative Heat Transfer in Glass Cooling Processes
(23 pages, 1998)

5. A. Klar, R. Wegener
A hierarchy of models for multilane vehicular traffic
Part I: Modeling
(23 pages, 1998)

Part II: Numerical and stochastic investigations
(17 pages, 1998)

6. A. Klar, N. Siedow
Boundary Layers and Domain Decomposition for Radiative Heat Transfer and Diffusion Equations: Applications to Glass Manufacturing Processes
(24 pages, 1998)

7. I. Choquet
Heterogeneous catalysis modelling and numerical simulation in rarified gas flows Part I: Coverage locally at equilibrium
(24 pages, 1998)

8. J. Ohser, B. Steinbach, C. Lang
Efficient Texture Analysis of Binary Images
(17 pages, 1998)

9. J. Orlik
Homogenization for viscoelasticity of the integral type with aging and shrinkage
(20 pages, 1998)

10. J. Mohring
Helmholtz Resonators with Large Aperture
(21 pages, 1998)

11. H. W. Hamacher, A. Schöbel
On Center Cycles in Grid Graphs
(15 pages, 1998)

12. H. W. Hamacher, K.-H. Küfer
Inverse radiation therapy planning - a multiple objective optimisation approach
(14 pages, 1999)

13. C. Lang, J. Ohser, R. Hilfer
On the Analysis of Spatial Binary Images
(20 pages, 1999)

14. M. Junk
On the Construction of Discrete Equilibrium Distributions for Kinetic Schemes
(24 pages, 1999)

15. M. Junk, S. V. Raghurame Rao
A new discrete velocity method for Navier-Stokes equations
(20 pages, 1999)

16. H. Neunzert
Mathematics as a Key to Key Technologies
(39 pages (4 PDF-Files), 1999)

17. J. Ohser, K. Sandau
Considerations about the Estimation of the Size Distribution in Wicksell's Corpuscle Problem
(18 pages, 1999)

18. E. Carrizosa, H. W. Hamacher, R. Klein, S. Nickel
Solving nonconvex planar location problems by finite dominating sets
Keywords: Continuous Location, Polyhedral Gauges, Finite Dominating Sets, Approximation, Sandwich Algorithm, Greedy Algorithm
(19 pages, 2000)

19. A. Becker
A Review on Image Distortion Measures
Keywords: Distortion measure, human visual system
(26 pages, 2000)

20. H. W. Hamacher, M. Labbé, S. Nickel, T. Sonneborn
Polyhedral Properties of the Uncapacitated Multiple Allocation Hub Location Problem
Keywords: integer programming, hub location, facility location, valid inequalities, facets, branch and cut
(21 pages, 2000)

21. H. W. Hamacher, A. Schöbel
Design of Zone Tariff Systems in Public Transportation
(30 pages, 2001)

22. D. Hietel, M. Junk, R. Keck, D. Teleaga
The Finite-Volume-Particle Method for Conservation Laws
(16 pages, 2001)

23. T. Bender, H. Hennes, J. Kalcsics, M. T. Melo, S. Nickel
Location Software and Interface with GIS and Supply Chain Management
Keywords: facility location, software development, geographical information systems, supply chain management
(48 pages, 2001)

24. H. W. Hamacher, S. A. Tjandra
Mathematical Modelling of Evacuation Problems: A State of Art
(44 pages, 2001)

25. J. Kuhnert, S. Tiwari
Grid free method for solving the Poisson equation
Keywords: Poisson equation, Least squares method, Grid free method
(19 pages, 2001)

26. T. Götz, H. Rave, D. Reinel-Bitzer, K. Steiner, H. Tiemeier
Simulation of the fiber spinning process
Keywords: Melt spinning, fiber model, Lattice Boltzmann, CFD
(19 pages, 2001)

27. A. Zemitis
On interaction of a liquid film with an obstacle
Keywords: impinging jets, liquid film, models, numerical solution, shape
(22 pages, 2001)

28. I. Ginzburg, K. Steiner
Free surface lattice-Boltzmann method to model the filling of expanding cavities by Bingham Fluids
Keywords: Generalized LBE, free-surface phenomena, interface boundary conditions, filling processes, Bingham viscoplastic model, regularized models
(22 pages, 2001)

29. H. Neunzert
»Denn nichts ist für den Menschen als Menschen etwas wert, was er nicht mit Leidenschaft tun kann«
Vortrag anlässlich der Verleihung des Akademiepreises des Landes Rheinland-Pfalz am 21.11.2001
Keywords: Lehre, Forschung, angewandte Mathematik, Mehrskalenanalyse, Strömungsmechanik
(18 pages, 2001)

30. J. Kuhnert, S. Tiwari
Finite pointset method based on the projection method for simulations of the incompressible Navier-Stokes equations
Keywords: Incompressible Navier-Stokes equations, Meshfree method, Projection method, Particle scheme, Least squares approximation
AMS subject classification: 76D05, 76M28
(25 pages, 2001)

31. R. Korn, M. Krekel
Optimal Portfolios with Fixed Consumption or Income Streams
Keywords: Portfolio optimisation, stochastic control, HJB equation, discretisation of control problems
(23 pages, 2002)

32. M. Krekel
Optimal portfolios with a loan dependent credit spread
Keywords: Portfolio optimisation, stochastic control, HJB equation, credit spread, log utility, power utility, non-linear wealth dynamics
(25 pages, 2002)

33. J. Ohser, W. Nagel, K. Schladitz
The Euler number of discretized sets – on the choice of adjacency in homogeneous lattices
Keywords: image analysis, Euler number, neighborhod relationships, cuboidal lattice
(32 pages, 2002)

34. I. Ginzburg, K. Steiner
Lattice Boltzmann Model for Free-Surface flow and Its Application to Filling Process in Casting

Keywords: Lattice Boltzmann models; free-surface phenomena; interface boundary conditions; filling processes; injection molding; volume of fluid method; interface boundary conditions; advection-schemes; upwind-schemes
(54 pages, 2002)

35. M. Günther, A. Klar, T. Materne, R. Wegener
Multivalued fundamental diagrams and stop and go waves for continuum traffic equations
Keywords: traffic flow, macroscopic equations, kinetic derivation, multivalued fundamental diagram, stop and go waves, phase transitions
(25 pages, 2002)

36. S. Feldmann, P. Lang, D. Prätzel-Wolters
Parameter influence on the zeros of network determinants
Keywords: Networks, Equicofactor matrix polynomials, Realization theory, Matrix perturbation theory
(30 pages, 2002)

37. K. Koch, J. Ohser, K. Schladitz
Spectral theory for random closed sets and estimating the covariance via frequency space
Keywords: Random set, Bartlett spectrum, fast Fourier transform, power spectrum
(28 pages, 2002)

38. D. d'Humières, I. Ginzburg
Multi-reflection boundary conditions for lattice Boltzmann models
Keywords: lattice Boltzmann equation, boudary condistions, bounce-back rule, Navier-Stokes equation
(72 pages, 2002)

39. R. Korn
Elementare Finanzmathematik
Keywords: Finanzmathematik, Aktien, Optionen, Portfolio-Optimierung, Börse, Lehrerweiterbildung, Mathematikunterricht
(98 pages, 2002)

40. J. Kallrath, M. C. Müller, S. Nickel
Batch Presorting Problems: Models and Complexity Results
Keywords: Complexity theory, Integer programming, Assigment, Logistics
(19 pages, 2002)

41. J. Linn
On the frame-invariant description of the phase space of the Folgar-Tucker equation
Key words: fiber orientation, Folgar-Tucker equation, injection molding
(5 pages, 2003)

42. T. Hanne, S. Nickel
A Multi-Objective Evolutionary Algorithm for Scheduling and Inspection Planning in Software Development Projects
Key words: multiple objective programming, project management and scheduling, software development, evolutionary algorithms, efficient set
(29 pages, 2003)

43. T. Bortfeld , K.-H. Küfer, M. Monz, A. Scherrer, C. Thieke, H. Trinkaus
Intensity-Modulated Radiotherapy - A Large Scale Multi-Criteria Programming Problem
Keywords: multiple criteria optimization, representative systems of Pareto solutions, adaptive triangulation, clustering and disaggregation techniques, visualization of Pareto solutions, medical physics, external beam radiotherapy planning, intensity modulated radiotherapy
(31 pages, 2003)

44. T. Halfmann, T. Wichmann
Overview of Symbolic Methods in Industrial Analog Circuit Design
Keywords: CAD, automated analog circuit design, symbolic analysis, computer algebra, behavioral modeling, system simulation, circuit sizing, macro modeling, differential-algebraic equations, index
(17 pages, 2003)

45. S. E. Mikhailov, J. Orlik
Asymptotic Homogenisation in Strength and Fatigue Durability Analysis of Composites
Keywords: multiscale structures, asymptotic homogenization, strength, fatigue, singularity, non-local conditions
(14 pages, 2003)

46. P. Domínguez-Marín, P. Hansen, N. Mladenovi´c , S. Nickel
Heuristic Procedures for Solving the Discrete Ordered Median Problem
Keywords: genetic algorithms, variable neighborhood search, discrete facility location
(31 pages, 2003)

47. N. Boland, P. Domínguez-Marín, S. Nickel, J. Puerto
Exact Procedures for Solving the Discrete Ordered Median Problem
Keywords: discrete location, Integer programming
(41 pages, 2003)

48. S. Feldmann, P. Lang
Padé-like reduction of stable discrete linear systems preserving their stability
Keywords: Discrete linear systems, model reduction, stability, Hankel matrix, Stein equation
(16 pages, 2003)

49. J. Kallrath, S. Nickel
A Polynomial Case of the Batch Presorting Problem
Keywords: batch presorting problem, online optimization, competetive analysis, polynomial algorithms, logistics
(17 pages, 2003)

50. T. Hanne, H. L. Trinkaus
knowCube for MCDM – Visual and Interactive Support for Multicriteria Decision Making
Key words: Multicriteria decision making, knowledge management, decision support systems, visual interfaces, interactive navigation, real-life applications.
(26 pages, 2003)

51. O. Iliev, V. Laptev
On Numerical Simulation of Flow Through Oil Filters
Keywords: oil filters, coupled flow in plain and porous media, Navier-Stokes, Brinkman, numerical simulation
(8 pages, 2003)

52. W. Dörfler, O. Iliev, D. Stoyanov, D. Vassileva
On a Multigrid Adaptive Refinement Solver for Saturated Non-Newtonian Flow in Porous Media
Keywords: Nonlinear multigrid, adaptive refinement, non-Newtonian flow in porous media
(17 pages, 2003)

53. S. Kruse
On the Pricing of Forward Starting Options under Stochastic Volatility
Keywords: Option pricing, forward starting options, Heston model, stochastic volatility, cliquet options
(11 pages, 2003)

54. O. Iliev, D. Stoyanov
Multigrid – adaptive local refinement solver for incompressible flows
Keywords: Navier-Stokes equations, incompressible flow, projection-type splitting, SIMPLE, multigrid methods, adaptive local refinement, lid-driven flow in a cavity
(37 pages, 2003)

55. V. Starikovicius
The multiphase flow and heat transfer in porous media
Keywords: Two-phase flow in porous media, various formulations, global pressure, multiphase mixture model, numerical simulation
(30 pages, 2003)

56. P. Lang, A. Sarishvili, A. Wirsen
Blocked neural networks for knowledge extraction in the software development process
Keywords: Blocked Neural Networks, Nonlinear Regression, Knowledge Extraction, Code Inspection
(21 pages, 2003)

57. H. Knaf, P. Lang, S. Zeiser
Diagnosis aiding in Regulation Thermography using Fuzzy Logic
Keywords: fuzzy logic,knowledge representation, expert system
(22 pages, 2003)

58. M. T. Melo, S. Nickel, F. Saldanha da Gama
Largescale models for dynamic multicommodity capacitated facility location
Keywords: supply chain management, strategic planning, dynamic location, modeling
(40 pages, 2003)

59. J. Orlik
Homogenization for contact problems with periodically rough surfaces
Keywords: asymptotic homogenization, contact problems
(28 pages, 2004)

60. A. Scherrer, K.-H. Küfer, M. Monz, F. Alonso, T. Bortfeld
IMRT planning on adaptive volume structures – a significant advance of computational complexity
Keywords: Intensity-modulated radiation therapy (IMRT), inverse treatment planning, adaptive volume structures, hierarchical clustering, local refinement, adaptive clustering, convex programming, mesh generation, multi-grid methods
(24 pages, 2004)

61. D. Kehrwald
Parallel lattice Boltzmann simulation of complex flows
Keywords: Lattice Boltzmann methods, parallel computing, microstructure simulation, virtual material design, pseudo-plastic fluids, liquid composite moulding
(12 pages, 2004)

62. O. Iliev, J. Linn, M. Moog, D. Niedziela, V. Starikovicius
On the Performance of Certain Iterative Solvers for Coupled Systems Arising in Discretization of Non-Newtonian Flow Equations
Keywords: Performance of iterative solvers, Preconditioners, Non-Newtonian flow
(17 pages, 2004)

63. R. Ciegis, O. Iliev, S. Rief, K. Steiner
On Modelling and Simulation of Different Regimes for Liquid Polymer Moulding

Keywords: Liquid Polymer Moulding, Modelling, Simulation, Infiltration, Front Propagation, non-Newtonian flow in porous media
(43 pages, 2004)

64. T. Hanne, H. Neu
Simulating Human Resources in Software Development Processes
Keywords: Human resource modeling, software process, productivity, human factors, learning curve
(14 pages, 2004)

65. O. Iliev, A. Mikelic, P. Popov
Fluid structure interaction problems in deformable porous media: Toward permeability of deformable porous media
Keywords: fluid-structure interaction, deformable porous media, upscaling, linear elasticity, stokes, finite elements
(28 pages, 2004)

66. F. Gaspar, O. Iliev, F. Lisbona, A. Naumovich, P. Vabishchevich
On numerical solution of 1-D poroelasticity equations in a multilayered domain
Keywords: poroelasticity, multilayered material, finite volume discretization, MAC type grid
(41 pages, 2004)

67. J. Ohser, K. Schladitz, K. Koch, M. Nöthe
Diffraction by image processing and its application in materials science
Keywords: porous microstructure, image analysis, random set, fast Fourier transform, power spectrum, Bartlett spectrum
(13 pages, 2004)

68. H. Neunzert
Mathematics as a Technology: Challenges for the next 10 Years
Keywords: applied mathematics, technology, modelling, simulation, visualization, optimization, glass processing, spinning processes, fiber-fluid interaction, trubulence effects, topological optimization, multicriteria optimization, Uncertainty and Risk, financial mathematics, Malliavin calculus, Monte-Carlo methods, virtual material design, filtration, bio-informatics, system biology
(29 pages, 2004)

69. R. Ewing, O. Iliev, R. Lazarov, A. Naumovich
On convergence of certain finite difference discretizations for 1D poroelasticity interface problems
Keywords: poroelasticity, multilayered material, finite volume discretizations, MAC type grid, error estimates
(26 pages,2004)

70. W. Dörfler, O. Iliev, D. Stoyanov, D. Vassileva
On Efficient Simulation of Non-Newtonian Flow in Saturated Porous Media with a Multigrid Adaptive Refinement Solver
Keywords: Nonlinear multigrid, adaptive renement, non-Newtonian in porous media
(25 pages, 2004)

71. J. Kalcsics, S. Nickel, M. Schröder
Towards a Unified Territory Design Approach – Applications, Algorithms and GIS Integration
Keywords: territory desgin, political districting, sales territory alignment, optimization algorithms, Geographical Information Systems
(40 pages, 2005)

72. K. Schladitz, S. Peters, D. Reinel-Bitzer, A. Wiegmann, J. Ohser
Design of acoustic trim based on geometric modeling and flow simulation for non-woven
Keywords: random system of fibers, Poisson line process, flow resistivity, acoustic absorption, Lattice-Boltzmann method, non-woven
(21 pages, 2005)

73. V. Rutka, A. Wiegmann
Explicit Jump Immersed Interface Method for virtual material design of the effective elastic moduli of composite materials
Keywords: virtual material design, explicit jump immersed interface method, effective elastic moduli, composite materials
(22 pages, 2005)

74. T. Hanne
Eine Übersicht zum Scheduling von Baustellen
Keywords: Projektplanung, Scheduling, Bauplanung, Bauindustrie
(32 pages, 2005)

75. J. Linn
The Folgar-Tucker Model as a Differetial Algebraic System for Fiber Orientation Calculation
Keywords: fiber orientation, Folgar–Tucker model, invariants, algebraic constraints, phase space, trace stability
(15 pages, 2005)

76. M. Speckert, K. Dreßler, H. Mauch, A. Lion, G. J. Wierda
Simulation eines neuartigen Prüfsystems für Achserprobungen durch MKS-Modellierung einschließlich Regelung
Keywords: virtual test rig, suspension testing, multibody simulation, modeling hexapod test rig, optimization of test rig configuration
(20 pages, 2005)

77. K.-H. Küfer, M. Monz, A. Scherrer, P. Süss, F. Alonso, A. S. A. Sultan, Th. Bortfeld, D. Craft, Chr. Thieke
Multicriteria optimization in intensity modulated radiotherapy planning
Keywords: multicriteria optimization, extreme solutions, real-time decision making, adaptive approximation schemes, clustering methods, IMRT planning, reverse engineering
(51 pages, 2005)

78. S. Amstutz, H. Andrä
A new algorithm for topology optimization using a level-set method
Keywords: shape optimization, topology optimization, topological sensitivity, level-set
(22 pages, 2005)

79. N. Ettrich
Generation of surface elevation models for urban drainage simulation
Keywords: Flooding, simulation, urban elevation models, laser scanning
(22 pages, 2005)

80. H. Andrä, J. Linn, I. Matei, I. Shklyar, K. Steiner, E. Teichmann
OPTCAST – Entwicklung adäquater Strukturoptimierungsverfahren für Gießereien Technischer Bericht (KURZFASSUNG)
Keywords: Topologieoptimierung, Level-Set-Methode, Gießprozesssimulation, Gießtechnische Restriktionen, CAE-Kette zur Strukturoptimierung
(77 pages, 2005)

81. N. Marheineke, R. Wegener
Fiber Dynamics in Turbulent Flows Part I: General Modeling Framework
Keywords: fiber-fluid interaction; Cosserat rod; turbulence modeling; Kolmogorov's energy spectrum; double-velocity correlations; differentiable Gaussian fields
(20 pages, 2005)

Part II: Specific Taylor Drag
Keywords: flexible fibers; k-ε turbulence model; fiber-turbulence interaction scales; air drag; random Gaussian aerodynamic force; white noise; stochastic differential equations; ARMA process
(18 pages, 2005)

82. C. H. Lampert, O. Wirjadi
An Optimal Non-Orthogonal Separation of the Anisotropic Gaussian Convolution Filter
Keywords: Anisotropic Gaussian filter, linear filtering, orientation space, nD image processing, separable filters
(25 pages, 2005)

83. H. Andrä, D. Stoyanov
Error indicators in the parallel finite element solver for linear elasticity DDFEM
Keywords: linear elasticity, finite element method, hierarchical shape functions, domain decom-position, parallel implementation, a posteriori error estimates
(21 pages, 2006)

84. M. Schröder, I. Solchenbach
Optimization of Transfer Quality in Regional Public Transit
Keywords: public transit, transfer quality, quadratic assignment problem
(16 pages, 2006)

85. A. Naumovich, F. J. Gaspar
On a multigrid solver for the three-dimensional Biot poroelasticity system in multilayered domains
Keywords: poroelasticity, interface problem, multigrid, operator-dependent prolongation
(11 pages, 2006)

86. S. Panda, R. Wegener, N. Marheineke
Slender Body Theory for the Dynamics of Curved Viscous Fibers
Keywords: curved viscous fibers; fluid dynamics; Navier-Stokes equations; free boundary value problem; asymptotic expansions; slender body theory
(14 pages, 2006)

87. E. Ivanov, H. Andrä, A. Kudryavtsev
Domain Decomposition Approach for Automatic Parallel Generation of Tetrahedral Grids
Key words: Grid Generation, Unstructured Grid, Delaunay Triangulation, Parallel Programming, Domain Decomposition, Load Balancing
(18 pages, 2006)

88. S. Tiwari, S. Antonov, D. Hietel, J. Kuhnert, R. Wegener
A Meshfree Method for Simulations of Interactions between Fluids and Flexible Structures
Key words: Meshfree Method, FPM, Fluid Structure Interaction, Sheet of Paper, Dynamical Coupling
(16 pages, 2006)

89. R. Ciegis , O. Iliev, V. Starikovicius, K. Steiner
Numerical Algorithms for Solving Problems of Multiphase Flows in Porous Media
Keywords: nonlinear algorithms, finite-volume method, software tools, porous media, flows
(16 pages, 2006)

90. D. Niedziela, O. Iliev, A. Latz
On 3D Numerical Simulations of Viscoelastic Fluids

Keywords: non-Newtonian fluids, anisotropic viscosity, integral constitutive equation
(18 pages, 2006)

91. A. Winterfeld
Application of general semi-infinite Programming to Lapidary Cutting Problems
Keywords: large scale optimization, nonlinear programming, general semi-infinite optimization, design centering, clustering
(26 pages, 2006)

92. J. Orlik, A. Ostrovska
Space-Time Finite Element Approximation and Numerical Solution of Hereditary Linear Viscoelasticity Problems
Keywords: hereditary viscoelasticity; kern approximation by interpolation; space-time finite element approximation, stability and a priori estimate
(24 pages, 2006)

93. V. Rutka, A. Wiegmann, H. Andrä
EJIIM for Calculation of effective Elastic Moduli in 3D Linear Elasticity
Keywords: Elliptic PDE, linear elasticity, irregular domain, finite differences, fast solvers, effective elastic moduli
(24 pages, 2006)

94. A. Wiegmann, A. Zemitis
EJ-HEAT: A Fast Explicit Jump Harmonic Averaging Solver for the Effective Heat Conductivity of Composite Materials
Keywords: Stationary heat equation, effective thermal conductivity, explicit jump, discontinuous coefficients, virtual material design, microstructure simulation, EJ-HEAT
(21 pages, 2006)

95. A. Naumovich
On a finite volume discretization of the three-dimensional Biot poroelasticity system in multilayered domains
Keywords: Biot poroelasticity system, interface problems, finite volume discretization, finite difference method
(21 pages, 2006)

96. M. Krekel, J. Wenzel
A unified approach to Credit Default Swaption and Constant Maturity Credit Default Swap valuation
Keywords: LIBOR market model, credit risk, Credit Default Swaption, Constant Maturity Credit Default Swap-method
(43 pages, 2006)

97. A. Dreyer
Interval Methods for Analog Circiuts
Keywords: interval arithmetic, analog circuits, tolerance analysis, parametric linear systems, frequency response, symbolic analysis, CAD, computer algebra
(36 pages, 2006)

98. N. Weigel, S. Weihe, G. Bitsch, K. Dreßler
Usage of Simulation for Design and Optimization of Testing
Keywords: Vehicle test rigs, MBS, control, hydraulics, testing philosophy
(14 pages, 2006)

99. H. Lang, G. Bitsch, K. Dreßler, M. Speckert
Comparison of the solutions of the elastic and elastoplastic boundary value problems
Keywords: Elastic BVP, elastoplastic BVP, variational inequalities, rate-independency, hysteresis, linear kinematic hardening, stop- and play-operator
(21 pages, 2006)

100. M. Speckert, K. Dreßler, H. Mauch
MBS Simulation of a hexapod based suspension test rig
Keywords: Test rig, MBS simulation, suspension, hydraulics, controlling, design optimization
(12 pages, 2006)

101. S. Azizi Sultan, K.-H. Küfer
A dynamic algorithm for beam orientations in multicriteria IMRT planning
Keywords: radiotherapy planning, beam orientation optimization, dynamic approach, evolutionary algorithm, global optimization
(14 pages, 2006)

102. T. Götz, A. Klar, N. Marheineke, R. Wegener
A Stochastic Model for the Fiber Lay-down Process in the Nonwoven Production
Keywords: fiber dynamics, stochastic Hamiltonian system, stochastic averaging
(17 pages, 2006)

103. Ph. Süss, K.-H. Küfer
Balancing control and simplicity: a variable aggregation method in intensity modulated radiation therapy planning
Keywords: IMRT planning, variable aggregation, clustering methods
(22 pages, 2006)

104. A. Beaudry, G. Laporte, T. Melo, S. Nickel
Dynamic transportation of patients in hospitals
Keywords: in-house hospital transportation, dial-a-ride, dynamic mode, tabu search
(37 pages, 2006)

105. Th. Hanne
Applying multiobjective evolutionary algorithms in industrial projects
Keywords: multiobjective evolutionary algorithms, discrete optimization, continuous optimization, electronic circuit design, semi-infinite programming, scheduling
(18 pages, 2006)

106. J. Franke, S. Halim
Wild bootstrap tests for comparing signals and images
Keywords: wild bootstrap test, texture classification, textile quality control, defect detection, kernel estimate, nonparametric regression
(13 pages, 2007)

107. Z. Drezner, S. Nickel
Solving the ordered one-median problem in the plane
Keywords: planar location, global optimization, ordered median, big triangle small triangle method, bounds, numerical experiments
(21 pages, 2007)

108. Th. Götz, A. Klar, A. Unterreiter, R. Wegener
Numerical evidance for the non-existing of solutions of the equations desribing rotational fiber spinning
Keywords: rotational fiber spinning, viscous fibers, boundary value problem, existence of solutions
(11 pages, 2007)

109. Ph. Süss, K.-H. Küfer
Smooth intensity maps and the Bortfeld-Boyer sequencer
Keywords: probabilistic analysis, intensity modulated radiotherapy treatment (IMRT), IMRT plan application, step-and-shoot sequencing
(8 pages, 2007)

110. E. Ivanov, O. Gluchshenko, H. Andrä, A. Kudryavtsev
Parallel software tool for decomposing and meshing of 3d structures
Keywords: a-priori domain decomposition, unstructured grid, Delaunay mesh generation
(14 pages, 2007)

111. O. Iliev, R. Lazarov, J. Willems
Numerical study of two-grid preconditioners for 1d elliptic problems with highly oscillating discontinuous coefficients
Keywords: two-grid algorithm, oscillating coefficients, preconditioner
(20 pages, 2007)

112. L. Bonilla, T. Götz, A. Klar, N. Marheineke, R. Wegener
Hydrodynamic limit of the Fokker-Planck-equation describing fiber lay-down processes
Keywords: stochastic dierential equations, Fokker-Planck equation, asymptotic expansion, Ornstein-Uhlenbeck process
(17 pages, 2007)

113. S. Rief
Modeling and simulation of the pressing section of a paper machine
Keywords: paper machine, computational fluid dynamics, porous media
(41 pages, 2007)

114. R. Ciegis, O. Iliev, Z. Lakdawala
On parallel numerical algorithms for simulating industrial filtration problems
Keywords: Navier-Stokes-Brinkmann equations, finite volume discretization method, SIMPLE, parallel computing, data decomposition method
(24 pages, 2007)

115. N. Marheineke, R. Wegener
Dynamics of curved viscous fibers with surface tension
Keywords: Slender body theory, curved viscous bers with surface tension, free boundary value problem
(25 pages, 2007)

116. S. Feth, J. Franke, M. Speckert
Resampling-Methoden zur mse-Korrektur und Anwendungen in der Betriebsfestigkeit
Keywords: Weibull, Bootstrap, Maximum-Likelihood, Betriebsfestigkeit
(16 pages, 2007)

117. H. Knaf
Kernel Fisher discriminant functions – a concise and rigorous introduction
Keywords: wild bootstrap test, texture classification, textile quality control, defect detection, kernel estimate, nonparametric regression
(30 pages, 2007)

118. O. Iliev, I. Rybak
On numerical upscaling for flows in heterogeneous porous media
Keywords: numerical upscaling, heterogeneous porous media, single phase flow, Darcy's law, multiscale problem, effective permeability, multipoint flux approximation, anisotropy
(17 pages, 2007)

119. O. Iliev, I. Rybak
On approximation property of multipoint flux approximation method

Keywords: Multipoint flux approximation, finite volume method, elliptic equation, discontinuous tensor coefficients, anisotropy
(15 pages, 2007)

120. O. Iliev, I. Rybak, J. Willems
On upscaling heat conductivity for a class of industrial problems
Keywords: Multiscale problems, effective heat conductivity, numerical upscaling, domain decomposition
(21 pages, 2007)

121. R. Ewing, O. Iliev, R. Lazarov, I. Rybak
On two-level preconditioners for flow in porous media
Keywords: Multiscale problem, Darcy's law, single phase flow, anisotropic heterogeneous porous media, numerical upscaling, multigrid, domain decomposition, efficient preconditioner
(18 pages, 2007)

122. M. Brickenstein, A. Dreyer
POLYBORI: A Gröbner basis framework for Boolean polynomials
Keywords: Gröbner basis, formal verification, Boolean polynomials, algebraic cryptoanalysis, satisfiability
(23 pages, 2007)

123. O. Wirjadi
Survey of 3d image segmentation methods
Keywords: image processing, 3d, image segmentation, binarization
(20 pages, 2007)

124. S. Zeytun, A. Gupta
A Comparative Study of the Vasicek and the CIR Model of the Short Rate
Keywords: interest rates, Vasicek model, CIR-model, calibration, parameter estimation
(17 pages, 2007)

125. G. Hanselmann, A. Sarishvili
Heterogeneous redundancy in software quality prediction using a hybrid Bayesian approach
Keywords: reliability prediction, fault prediction, non-homogeneous poisson process, Bayesian model averaging
(17 pages, 2007)

126. V. Maag, M. Berger, A. Winterfeld, K.-H. Küfer
A novel non-linear approach to minimal area rectangular packing
Keywords: rectangular packing, non-overlapping constraints, non-linear optimization, regularization, relaxation
(18 pages, 2007)

127. M. Monz, K.-H. Küfer, T. Bortfeld, C. Thieke
Pareto navigation – systematic multi-criteria-based IMRT treatment plan determination
Keywords: convex, interactive multi-objective optimization, intensity modulated radiotherapy planning
(15 pages, 2007)

128. M. Krause, A. Scherrer
On the role of modeling parameters in IMRT plan optimization
Keywords: intensity-modulated radiotherapy (IMRT), inverse IMRT planning, convex optimization, sensitivity analysis, elasticity, modeling parameters, equivalent uniform dose (EUD)
(18 pages, 2007)

129. A. Wiegmann
Computation of the permeability of porous materials from their microstructure by FFF-Stokes
Keywords: permeability, numerical homogenization, fast Stokes solver
(24 pages, 2007)

130. T. Melo, S. Nickel, F. Saldanha da Gama
Facility Location and Supply Chain Management – A comprehensive review
Keywords: facility location, supply chain management, network design
(54 pages, 2007)

131. T. Hanne, T. Melo, S. Nickel
Bringing robustness to patient flow management through optimized patient transports in hospitals
Keywords: Dial-a-Ride problem, online problem, case study, tabu search, hospital logistics
(23 pages, 2007)

132. R. Ewing, O. Iliev, R. Lazarov, I. Rybak, J. Willems
An efficient approach for upscaling properties of composite materials with high contrast of coefficients
Keywords: effective heat conductivity, permeability of fractured porous media, numerical upscaling, fibrous insulation materials, metal foams
(16 pages, 2008)

133. S. Gelareh, S. Nickel
New approaches to hub location problems in public transport planning
Keywords: integer programming, hub location, transportation, decomposition, heuristic
(25 pages, 2008)

134. G. Thömmes, J. Becker, M. Junk, A. K. Vaikuntam, D. Kehrwald, A. Klar, K. Steiner, A. Wiegmann
A Lattice Boltzmann Method for immiscible multiphase flow simulations using the Level Set Method
Keywords: Lattice Boltzmann method, Level Set method, free surface, multiphase flow
(28 pages, 2008)

135. J. Orlik
Homogenization in elasto-plasticity
Keywords: multiscale structures, asymptotic homogenization, nonlinear energy
(40 pages, 2008)

136. J. Almquist, H. Schmidt, P. Lang, J. Deitmer, M. Jirstrand, D. Prätzel-Wolters, H. Becker
Determination of interaction between MCT1 and CAII via a mathematical and physiological approach
Keywords: mathematical modeling; model reduction; electrophysiology; pH-sensitive microelectrodes; proton antenna
(20 pages, 2008)

137. E. Savenkov, H. Andrä, O. Iliev
An analysis of one regularization approach for solution of pure Neumann problem
Keywords: pure Neumann problem, elasticity, regularization, finite element method, condition number
(27 pages, 2008)

138. O. Berman, J. Kalcsics, D. Krass, S. Nickel
The ordered gradual covering location problem on a network
Keywords: gradual covering, ordered median function, network location
(32 pages, 2008)

139. S. Gelareh, S. Nickel
Multi-period public transport design: A novel model and solution approaches
Keywords: Integer programming, hub location, public transport, multi-period planning, heuristics
(31 pages, 2008)

140. T. Melo, S. Nickel, F. Saldanha-da-Gama
Network design decisions in supply chain planning
Keywords: supply chain design, integer programming models, location models, heuristics
(20 pages, 2008)

141. C. Lautensack, A. Särkkä, J. Freitag, K. Schladitz
Anisotropy analysis of pressed point processes
Keywords: estimation of compression, isotropy test, nearest neighbour distance, orientation analysis, polar ice, Ripley's K function
(35 pages, 2008)

142. O. Iliev, R. Lazarov, J. Willems
A Graph-Laplacian approach for calculating the effective thermal conductivity of complicated fiber geometries
Keywords: graph laplacian, effective heat conductivity, numerical upscaling, fibrous materials
(14 pages, 2008)

143. J. Linn, T. Stephan, J. Carlsson, R. Bohlin
Fast simulation of quasistatic rod deformations for VR applications
Keywords: quasistatic deformations, geometrically exact rod models, variational formulation, energy minimization, finite differences, nonlinear conjugate gradients
(7 pages, 2008)

144. J. Linn, T. Stephan
Simulation of quasistatic deformations using discrete rod models
Keywords: quasistatic deformations, geometrically exact rod models, variational formulation, energy minimization, finite differences, nonlinear conjugate gradients
(9 pages, 2008)

145. J. Marburger, N. Marheineke, R. Pinnau
Adjoint based optimal control using mesh-less discretizations
Keywords: Mesh-less methods, particle methods, Eulerian-Lagrangian formulation, optimization strategies, adjoint method, hyperbolic equations
(14 pages, 2008

146. S. Desmettre, J. Gould, A. Szimayer
Own-company stockholding and work effort preferences of an unconstrained executive
Keywords: optimal portfolio choice, executive compensation
(33 pages, 2008)

147. M. Berger, M. schröder, K.-H. Küfer
A constraint programming approach for the two-dimensional rectangular packing problem with orthogonal orientations
Keywords: rectangular packing, orthogonal orientations non-overlapping constraints, constraint propagation
(13 pages, 2008)

148. K. Schladitz, C. Redenbach, T. Sych, M. Godehardt

Microstructural characterisation of open foams using 3d images

Keywords: virtual material design, image analysis, open foams
(30 pages, 2008)

149. E. Fernández, J. Kalcsics, S. Nickel, R. Ríos-Mercado

A novel territory design model arising in the implementation of the WEEE-Directive

Keywords: heuristics, optimization, logistics, recycling
(28 pages, 2008)

150. H. Lang, J. Linn

Lagrangian field theory in space-time for geometrically exact Cosserat rods

Keywords: Cosserat rods, geometrically exact rods, small strain, large deformation, deformable bodies, Lagrangian field theory, variational calculus
(19 pages, 2009)

151. K. Dreßler, M. Speckert, R. Müller, Ch. Weber

Customer loads correlation in truck engineering

Keywords: Customer distribution, safety critical components, quantile estimation, Monte-Carlo methods
(11 pages, 2009)

152. H. Lang, K. Dreßler

An improved multiaxial stress-strain correction model for elastic FE postprocessing

Keywords: Jiang's model of elastoplasticity, stress-strain correction, parameter identification, automatic differentiation, least-squares optimization, Coleman-Li algorithm
(6 pages, 2009)

153. J. Kalcsics, S. Nickel, M. Schröder

A generic geometric approach to territory design and districting

Keywords: Territory design, districting, combinatorial optimization, heuristics, computational geometry
(32 pages, 2009)

154. Th. Fütterer, A. Klar, R. Wegener

An energy conserving numerical scheme for the dynamics of hyperelastic rods

Keywords: Cosserat rod, hyperealstic, energy conservation, finite differences
(16 pages, 2009)

155. A. Wiegmann, L. Cheng, E. Glatt, O. Iliev, S. Rief

Design of pleated filters by computer simulations

Keywords: Solid-gas separation, solid-liquid separation, pleated filter, design, simulation
(21 pages, 2009)

156. A. Klar, N. Marheineke, R. Wegener

Hierarchy of mathematical models for production processes of technical textiles

Keywords: Fiber-fluid interaction, slender-body theory, turbulence modeling, model reduction, stochastic differential equations, Fokker-Planck equation, asymptotic expansions, parameter identification
(21 pages, 2009)